



Review

Chitosan-derived hydrothermally carbonized materials and its applications: A review of recent literature

Hani Ababneh, B.H. Hameed*

Department of Chemical Engineering, College of Engineering, Qatar University, P.O Box: 2713, Doha, Qatar



ARTICLE INFO

Keywords:

Chitosan
Hydrothermal carbonization
Wastewater treatment
CO₂ capture
Supercapacitors
Catalyst
Biosensing

ABSTRACT

Chitosan (CS) is a linear polysaccharide biopolymer, one of the most abundant biowastes in the environment. This makes chitosan a potential material for a wide range of applications. To improve CS's properties, chitosan has to be chemically modified. Hydrothermal carbonization (HTC) is a sustainable process for converting chitosan to solid carbonized material. This article presents a review on the applications of hydrothermally treated chitosan in different fields such as water treatment, heavy metals adsorption, carbon dioxide capturing, solar cells, energy storage, biosensing, supercapacitors, and catalysis. Moreover, this review covers the impact of HTC process parameters on the properties of the produced carbon material. The diversity of applications indicates the great possibilities and multifunctionality of hydrothermally carbonized chitosan and its derivatives. The utilization of HTC-CS is expected to further expand as a result of the movement toward sustainable, environmentally-friendly resources. Thus, this review also recommends a few suggestions to improve the properties of HTC chitosan and its comprehensive applications.

1. Introduction

The negative impacts of the industrial revolution and modern industries on the environment have encouraged the scientific community to search for more sustainable and environmentally benign resources and chemicals. Biomass has attracted much attention in the last two decades as a green and sustainable resource for different applications [1–4]. Among those environmentally friendly resources is chitosan. Chitosan is a linear polysaccharide biopolymer with main structural units of 2-amino-2-deoxy-D-glucopyranose which are bonded by 1,4-glycosidic connections. [5]. Fig. 1 shows the chemical structure of chitosan [6].

Chitosan is sourced from chitin, which is the second most abundant form of polymerized carbon in nature after cellulose [7]. It is estimated that each year live organisms produce 10 billion tons of chitin [8]. The main sources to obtain chitin are the crab or shrimp shells and fungal mycelia, those by products are processed to produce the white powder of chitin [9]. Chitosan is prepared by deacetylation and depolymerization of chitin by 40–50% aqueous alkali solution at 100–160 °C for 1–3 h.

Chitosan is biocompatible, biodegradable and non-toxic polymer making environmentally friendly and safe for biomedical applications [10–12], biocatalysts [13], food packaging and treatment [14,15],

bioprinting [16], and other applications [17,18]. One of the main advantages of the chitosan is its high nitrogen content (6.89%) [9]; to clarify, the reactivity of the amino group present in the chitosan allows for different chemical reactions and modifications hence, expanding the possibilities and applications for the chitosan [5]. In addition to the above-mentioned advantages, chitosan advantages include its hydrophilicity, crystallinity, ionic conductivity and high viscosity [5].

Since chitosan can be easily processed into different forms such as sponges, gels, beads, scaffolds, micro and nanoparticles [19]. Due to its advantages, chitosan and chitosan derived materials have found their way into many applications; they are used in water treatment, biosensors, pharmaceuticals, biomedicine, paper production, antiseptic dyes, biochemistry, preservatives materials, cosmetic, food additives, agricultural fields [20,21], and flame retardants [22]. Many synthesis techniques have been widely used to produce carbon materials from chitosan. They may be used alone or in combination with each other, they include hydrothermal carbonization (HTC), solvothermal treatment, microwave-assisted treatment, and pyrolysis [23].

Hydrothermal carbonization process (HTC) is one of many techniques used to process chitosan and convert it to solid carbonized material. HTC process is conducted at relatively mild conditions (low temperatures, neutral or acidic solutions) which make it a sustainable

* Corresponding author.

E-mail address: b.hammadi@qu.edu.qa (B.H. Hameed).

<https://doi.org/10.1016/j.ijbiomac.2021.06.161>

Received 23 April 2021; Received in revised form 21 June 2021; Accepted 24 June 2021

Available online 29 June 2021

0141-8130/© 2021 The Authors. Published by Elsevier B.V. This is an open access article under the CC BY license (<http://creativecommons.org/licenses/by/4.0/>).

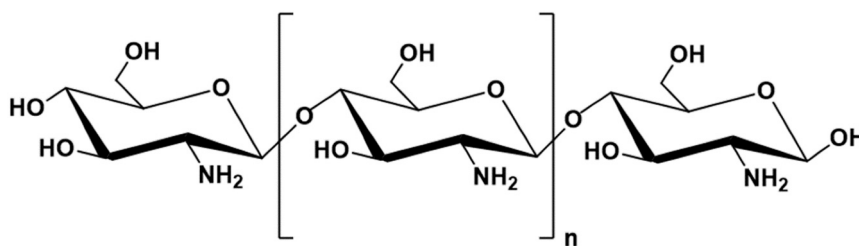


Fig. 1. Chemical structure of chitosan [6].

process and attractive for processing chitosan [3], and biomass [4,24]. HTC process can either be accomplished by conventional heating or by microwave assisted heating [25,26].

Chitosan-derived hydrothermally carbonized materials have been recently in the focus of the research. This due to its advantages; prepared from renewable sources, their surface characteristics are easy to modify, and they are cheap to produce. Furthermore, they are biocompatible, sustainable, and have no toxic residuals, thus opening the way to utilize them in different and multiple applications [1]. However, chitosan is highly susceptible to the solution pH value, hence it can either form gel or dissolve based on the pH values [27], thus it is really important to take that into account during the preparation of carbon materials from chitosan.

Adolfsson et al. reviewed the hydrothermally carbonized materials that originated from cellulose. The review covered the new applications of these materials and their properties [1]. Sharma et al. reviewed a wider range of bio sourced carbonized materials and the parameters which influence the carbonization process [28]. Annu and Raja reviewed the application and properties of chitosan hydrogels usage for electrochemical sensors in various fields [21]. Hammi et al. have recently reviewed the preparation methods of different nitrogen-containing carbon materials sourced from chitosan, and the applications offered by these materials in the field of catalysis [23]. In the field of water treatment, Ahmed et al. have discussed the latest progress of utilizing chitosan-derived carbonaceous materials for the adsorption of water pollutants. The review also covered the performance of those adsorbents and the possibilities of regenerating and reusing them [29]. A more specific review is covering the usage of chitosan-based nanocomposite for removal of the toxic Cr (VI) from solution and wastewater. The review focuses on the adsorption capacity, kinetics and adsorption isotherm of Cr (VI) adsorption [30]. Varma has discussed the sustainable utilization of carbonaceous materials in the chemical and environmental applications, the carbonaceous materials in consideration are bio-derived and renewable, they include cellulose, chitin, and chitosan [31].

The objective of this review is to cover the chitosan-derived hydrothermally carbonized materials and their applications. Furthermore, it covers the recent progress in the applications and utilization of the carbonized materials in the fields of environmental applications, energy applications, supercapacitors, biosensing, and catalysis.

2. Chitosan structure and properties

Unless in special conditions, chitosan is never 100% deacetylated [8]. The usual chitosan deacetylation level is between 70% and 95% [9]. The properties of chitosan depend on its molecular weight, purity, and the sequence of the amino and the acetamido groups content. The properties of chitosan are affected by its molecular weight and its degree of deacetylation. The average molecular weight of chitin is 1.03×10^6 to 2.5×10^6 g/mol, however after the *N*-deacetylation reaction, hence producing chitosan decreases to 1×10^5 to 5×10^5 g/mol [32].

The ratio of 2-acetamido-2-deoxy-D-glucopyranose to 2-amino-2-deoxy-D-glucopyranose structural units is known as degree of *N*-acetylation. This ratio has a noticeable impact on the chitosan solubility and solution properties [9]. Among the main properties of chitosan is its

high Nitrogen content [33], nitrogen in chitosan is found as C–N group and –NH₂ side group [34], those Nitrogen groups improves the activity of the chitosan and expands its applications into different fields.

3. Hydrothermal carbonization (HTC) process

Hydrothermal carbonization process also known as wet torrefaction was first discovered in 1913 [35]. HTC is a thermo-chemical conversion process in which biomass material is converted to solid carbonized material, thus mimicking the coalification process in nature [4]. Few decades later HTC process was mainly used for the degradation of organic materials, production of basic chemicals, and production of liquid and gaseous fuels [36], however in the recent years, this technology gained the interests of the researchers as method to produce solid hydrochar, and more recently, as technique to synthesize nano- and micro-size carbon particles [35,37,38]. Compared to the other biomass utilization techniques such as pyrolysis, HTC has the advantage of being able to utilize high-moisture content biomass as a feedstock, plus it is safer since it produces less harmful gases such as CO and CO₂. In addition to that, solids produced by HTC have many surface oxygen groups, hence they are less prone to auto-ignition [35]. The carbonized materials produced by the HTC process have a higher energy content than the feedstock used in the to produce them while at same time and lower O/C and H/C ratios than the feedstock [35].

Chitosan-derived hydrothermally carbonized materials can be produced as carbon dots. Carbon dots have attracted much attention in the last few decades [39]. Carbon dots are nanoparticles with the size of less than 10 nm, and because of their unique and exceptional properties such as nontoxicity and biocompatibility, they became attractive for application several fields such as biosensing, delivery of drugs and genes, catalysis, and solar cells [39–42]. One of the popular methods to prepare carbon dots is the bottom-up methods, HTC is one of them [43], in case of the same precursor, the limiting factors in determining the size of the carbon dots are temperature, reaction time, and the pH of HTC solution. Miao et al. have concluded that higher preparation temperatures results in larger size carbon dots [44], higher temperatures lead to higher carbonization degrees, therefore larger particle size. Similarly, longer reaction time produces carbon dots with higher carbonization levels and larger particle sizes [43]. Lower pH values improves the carbonization degree, which in results produces larger particle sizes [45,46].

Chitosan-derived hydrothermally carbonized materials also come as clay nanocomposites [47], codoped porous carbon materials [48], [49], aerogels [50] and more. HTC process is conducted in autogenous pressure and relatively mild conditions. It requires neutral or acidic aqueous solutions, and temperatures typically between 180 and 260 °C [1]. Furthermore, HTC requires long residence times 5 mins to 12 h and heating rate of 5–10 °C/min [35], Section 4.2 discusses the impact of these parameters on the properties and morphology of the products and the products distribution [37]. The products of HTC are classified according to their physical phase: solid, aqueous solution, and small volume of gas (mainly CO₂) [3], with the solid residue being the main product [51]. The type of the feedstock and process conditions impact the distribution and properties of the products [52].

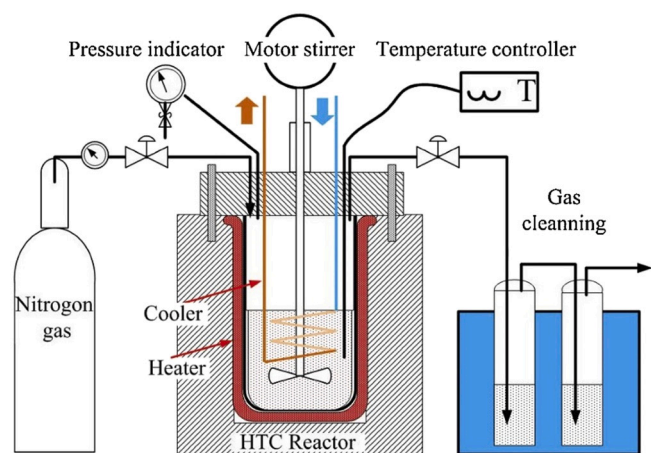


Fig. 2. Typical setup of autoclave reactor used for HTC process [56].

3.1. Process chemistry

During the HTC process many reactions take place consequently and may occur simultaneously [38]. The mechanisms and kinetics involved in the process are not fully understood yet [2]. HTC process involves hydrolysis, dehydration, decarboxylation, aromatization, and recondensation reactions. Since the hydrolysis reaction has the lowest activation energy among the mentioned reactions, the HTC is considered governed by the hydrolysis reaction [2]. In the hydrolysis reaction ester and ether bonds between the biomass building blocks are broken down into different fragments and intermediates [53]. Reaction (1) shows an example of the dehydration reaction of glucose [54]. Since dehydration and decarboxylation degrade carboxyl and carbonyl groups and release CO_2 and CO they result in decreasing H/C and O/C ratios [2]. Following that, intermediates from the previous reactions react again to produce larger molecules. Finally, aromatization reactions will combine the larger molecules together forming a stable aromatic polymer structure [38].



The two most common reactors used for the HTC process are pressurized Parr reactor and autoclave reactors. Autoclave reactors are usually stainless steel or Teflon-lined [55]. Batch type reactors are the most widely used in the literature [2]. Fig. 2 shows a typical setup of HTC autoclave reactor [56]. The heat is transferred from the heat source of the reactor through the reactor walls reaching the reactor content i.e.

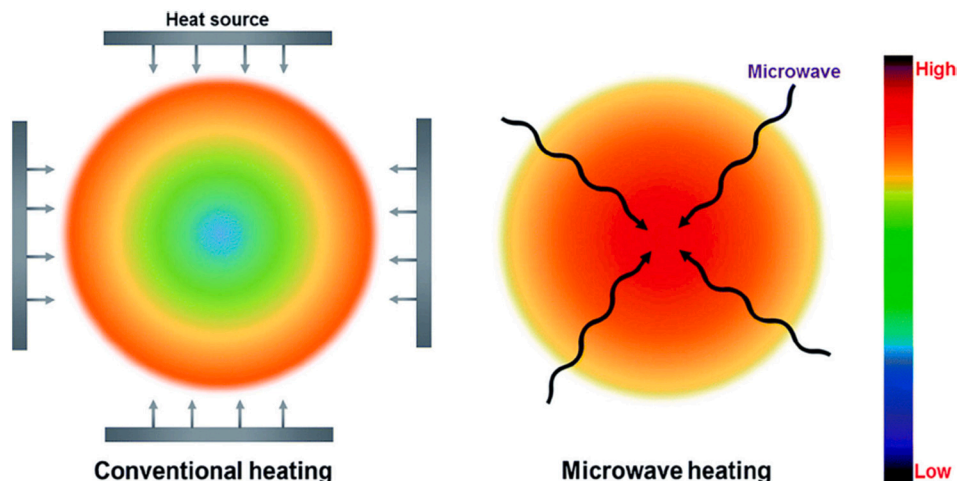


Fig. 3. Difference between microwave and conventional heating [60].

biomass chitosan [57].

Despite the advantages of conventional heating, it has many drawbacks which includes heat losses, side reactions, long residence time, and the difficulty in controlling the process [58]. Microwave heating has emerged as a solution for those shortcomings, in this method heat is generated by electromagnetic irradiation in a specific range of frequency [59], which is equivalent to wavelengths between 1×10^{-2} to 1 m [57]. Microwave heating offers many advantages over conventional heating; lower reaction times, higher reaction yield, more energy efficient (cheaper), and provides homogeneous heating. Fig. 3 illustrates the difference between conventional and microwave heating [60]. While the conventional heating methods requires several hours to reach the desired products, microwave heating can complete the same job in a few minutes [61]. Fig. 4 shows the typical setup for microwave-assisted HTC reactor [62].

Jia et al. [63] through studying the FTIR spectra of the precursor chitosan and HTC-treated one, found that the molecular hydrogen bonding (in $-\text{OH}$ and $-\text{NH}_2$) got weaker after the HTC reaction of chitosan, thus indicating that the main active sites to form hydrogen bonds were nitrogen from the amino groups, oxygen from chitosan acetyl amino groups, and the glycosidic bonds of chitosan. In addition to that, concluded that the electrostatic force does exist between the protonated amino groups in chitosan and some negatively charged atoms or groups. Therefore, impacting the pore structure and morphology of the resulted materials.

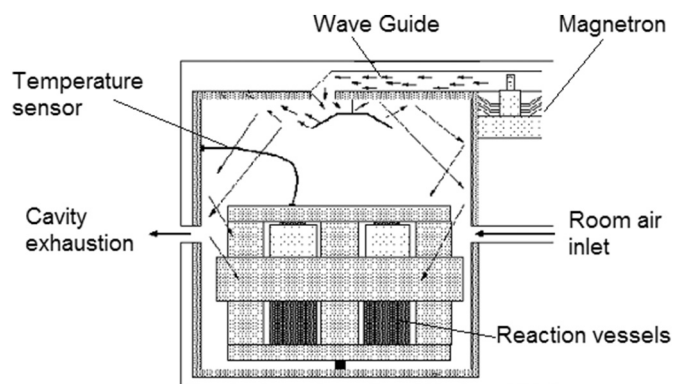


Fig. 4. Typical setup of microwave-assisted reactor used for HTC process [62].

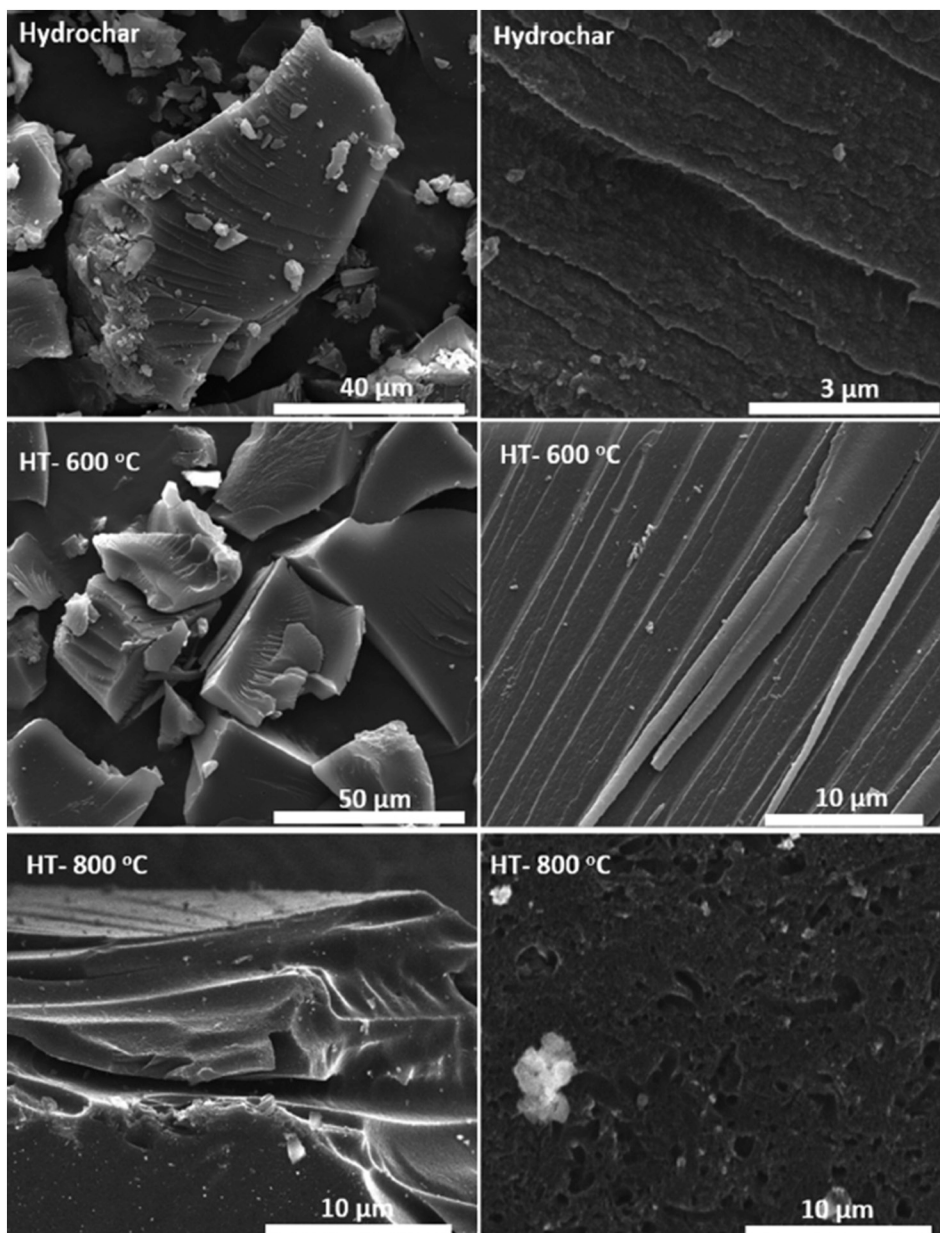


Fig. 5. SEM images for hydrochar and heat-treated carbons at different temperatures [65].

3.2. Parameters affecting the hydrothermal carbonization of chitosan

3.2.1. Effect of temperature

Temperature is the critical factor impacting the HTC process, and by increasing the temperature more energy is available to disintegrate the intermolecular bonds in the biomass (chitosan) [2]. Elevating the temperature will release more volatile materials, thus increasing the gaseous and liquids products over the solid products [28]. Shen et al. have varied the temperature of the HTC process of chitosan (140–220 °C) and noticed a decrease in the reaction yield from 78.8% to 35.2% [64]. In a different study, Castro et al. [65] studied the impact of post HTC thermal treatment on the products structural transformations of chitosan (200 to 800 °C). A higher post treatment temperature would increase the graphitization degree of the carbonaceous materials. However, it would deform the structure of the graphite. Furthermore, raising the temperature up to 600 °C increases the specific surface area of the graphitic-type structure before a total failure of this structure once the temperature exceeds 700 °C. Fig. 5 shows the scanning electron microscope

(SEM) images of the thermally treated carbons at 600 and 800 °C [65].

3.2.2. Effect of residence time

Time is another crucial factor affecting the HTC process, longer reaction time will result in more severe reactions [3]. Therefore, higher conversion rates [66]. Solid content decreases with increasing residence time although the impact of time is smaller than temperature [3]. This was proved by Simsir et al., who found that increasing the residence time from 6 to 30 h resulted in a slight decrease in the recovered solid mass yields for chitosan. The reason for that is that gasification reactions dominate at long reaction time, thus resulting in less carbon, while there was not noticeable change in the O/C ratios of products when residence time exceeds 12 h, after 18 h of reactions it was noticed that chitosan produced dense and uniform spheres with a diameter of 42 nm [67]. Chagas et al. found that increasing the HTC reaction time would increase carbon weight content of chitosan, while decreasing the O/C ratios in the resulting material [68]. Laginhas et al. [69] have found that at the same temperature, increasing the reaction time from 8 to 12 to 24 h

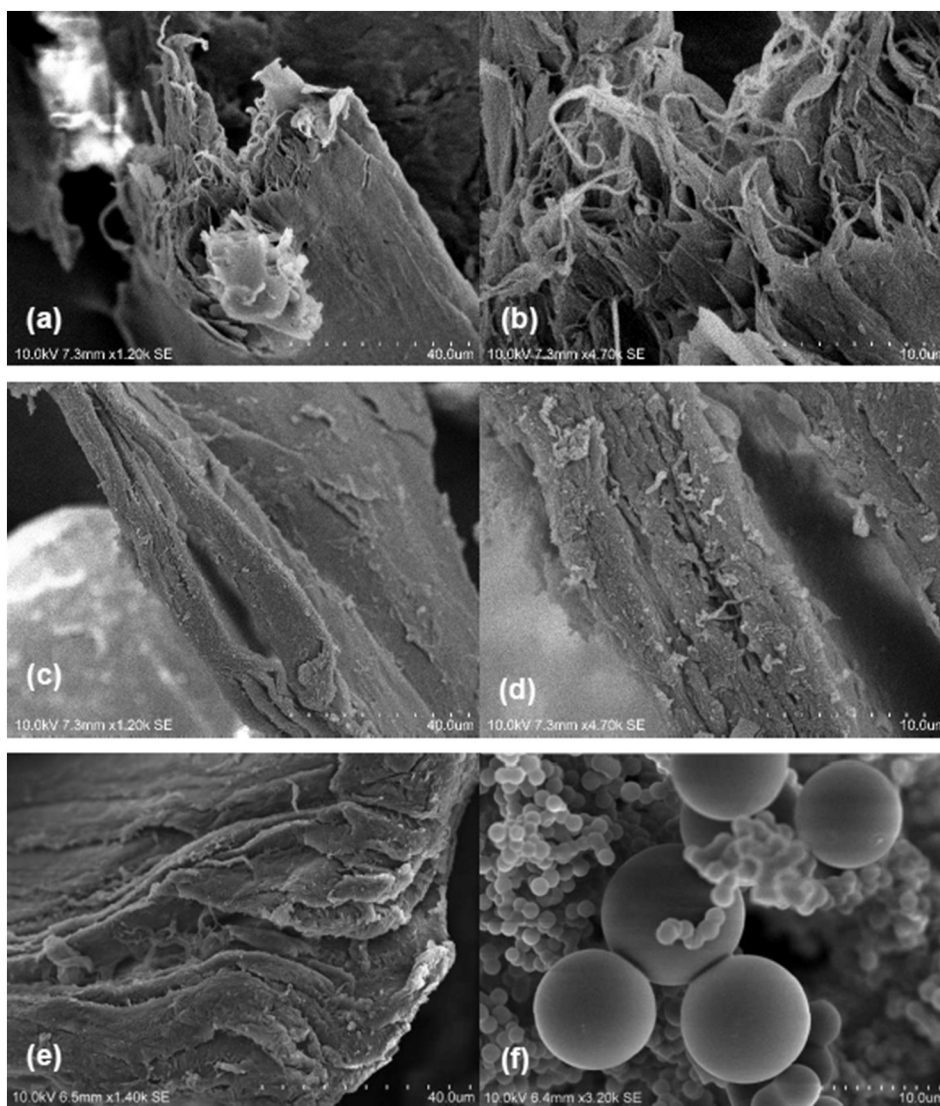


Fig. 6. SEM images for samples treated at 200 °C for 8 h ((a) and (b)), 12 h ((c) and (d)) and 24 h ((e) and (f)) [69].

would produce a mixture of shape regions; sphere-like and structure close to original chitosan structure as shown in Fig. 6, HTC process tends to produce sphere-like structure, thus more time allows higher levels of degradation of the original structure to spherical shapes [70,71]. In addition, it was found that the HTC process results in increasing the nitrogen content within the structure of the hydrothermal carbons, furthermore, oxygen content decreases with time.

4. Applications of chitosan-derived hydrothermally carbonized materials

4.1. Environmental applications

Because of the advantages carbonaceous materials sourced from chitosan offer, they have found their way into many environmental applications, which include wastewater treatment [72], heavy metals adsorption [73], and CO₂ capturing [74].

4.1.1. Wastewater treatment

Dye is a byproduct of many industries, small amounts of it in the wastewater is undesirable [75]. The current chemical and biological methods used to remove them are effective, however they produce a lot of byproducts [76]. To overcome this issue, natural physical adsorbents

are used; they are cheap, abundant, and environmentally safe [77–79]. For example, Zhou et al. have synthesized a nanomaterial using chitosan as precursors using the HTC method [47], the new adsorbent is attapulgite clay[®] carbonized chitosan (ATP@CCS). This new nanocomposite was used to remove methylene blue (MB) from wastewater. Based on the Langmuir adsorption isotherm, the ATP@CCS has a maximum adsorption capacity of 215.73 mg/g at 318.15 K. In addition, the prepared adsorbent has an outstanding reusability.

Another novel nanomaterial sourced from chitosan (Fe₃O₄@SiO₂@CCS porous magnetic microspheres) was prepared and used for dye removal [72]. This magnetic carbonaceous adsorbent was prepared by using HTC, microfluidic, ionic crosslinking methods. The produced adsorbent was tested for methylene blue (MB) methyl orange (MO), and Rhodamine B (RhB) removal. The maximum adsorption capacity for RhB was 191.57 mg/g at 25 °C. Fe₃O₄@SiO₂@CCS microspheres advantages are their excellent reusability, and ease of separating them from the solution using magnetic field. Operating at room temperature with neutral solution pH = 7, A slightly lower adsorption capacity for methylene blue (MB) (153.37 mg/g) was achieved using carbon-coated polyacrylonitrile nanofibers (oPAN@C) [80], however, adsorption efficiency remained high even after 5 cycles.

Feng et al. have studied the removal of diclofenac sodium (DCF) from wastewater at room temperature. To accomplish that, nanographene

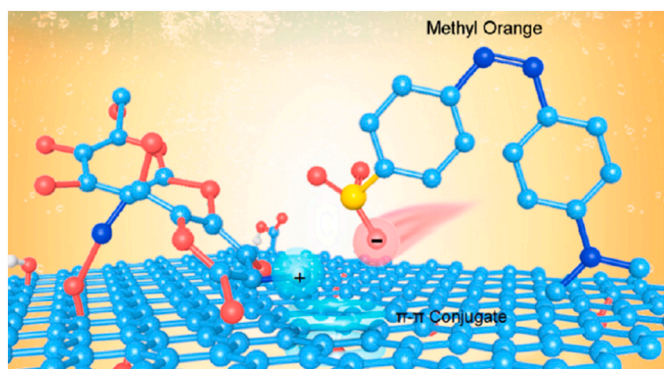


Fig. 7. Illustration of the adsorption process of methyl orange by the composite aerogel [82].

oxide (nGO)-type carbon dots were used as an enhancer in chitosan hydrogel adsorbents [61]. nGO were prepared by the HTC assisted microwave process. Macroporous CS/nGO hybrid hydrogels have achieved 100% removal of DCF in 5 h. It is believed that the improved adsorption performance in the previous studies is attributed to electrostatic interactions and hydrogen bonding. This was confirmed by another study

[81], where commercial chitosan was used to synthesize chitosan-based hydrochar (CCH) adsorbent using HTC process. The maximum adsorption capacity of methyl orange (MO) using CCH was 271.32 mg/g at solution pH 4 and temperature of 310 K. Zhu et al. used Chitosan—graphene oxide composite aerogel as adsorbent for methyl orange (MO) at room temperature [82]. The aerogel can adsorb as high as 97.2% of MO from the solution (48.6 mg/g). However, this is achieved in acidic conditions (pH = 1). At a higher pH values the adsorption efficiency decreases significantly. Fig. 7 illustrates the process of adsorption of methyl orange by the composite aerogel [82].

4.1.2. Heavy metals adsorption

Heavy metals such as Cr, Cd, Ni, Pb etc. have a harmful impact on aquatic organisms, and human's health. This is a result of their high toxicity, carcinogenicity, and bioaccumulation. Thus, it is important to remove them from the environmental systems [83]. Similar to dye removal from water, chitosan functional groups (amino and hydroxyl groups) make it an excellent selective adsorbent for removal of heavy metals [84]. Carbonaceous materials are more stable in acidic solutions than chitosan. Therefore, the HTC process is important in synthesizing adsorbents for heavy metals from water [85]. To illustrate, Wang et al. [73] synthesized a dual-core Fe_2O_3 @carbon microspheres for the removal of Cu ions from water. It was found that the adsorption

Table 1

Summary of studies in environmental applications of chitosan-sourced carbon materials.

Carbon material type	Preparation conditions	Application	Particle size (nm)	Polar groups	S_{BET} (m^2/g)	Results	Ref.
Amino-functionalized attapulgite clay nanoparticle adsorbent	HTC: 180 °C for 24 h	Methylene Blue (MB) removal from wastewater	Rod like nanostructure: Diameter: 40–80 length of 200–1000	O, N	80.65	Maximum adsorption capacity of 215.73 mg/g at 318.15 K	[47]
Fe_3O_4 @ SiO_2 @CCS porous magnetic microspheres	HTC: 200 °C for 5–24 h	Methylene blue (MB) methyl orange (MO), and Rhodamine B (RhB) removal from water	500–600 μm	O, N, Si, Fe	107.57	Maximum adsorption capacity for RhB was 191.57 mg/g at 25 °C	[72]
Nanographene oxide carbon dots	HTC: 200 °C for 2 h (microwave) HTC carbonized: 90 °C for 1 h	Removal of diclofenac sodium (DCF) from wastewater	60–70	O, N	–	100% removal of DCF in 5 h	[61]
Hydrochar adsorbent	HTC: 180 °C for 12 h	Methyl orange removal from aqueous solutions	–	O, N	12.65	Methyl orange (MO) 271.32 mg/g at pH 4 and 310 K	[81]
Carboxylic-functional carbon-coated polyacrylonitrile nanofibers (oPAN@C)	HTC: 180 °C for 8 h.	Methylene Blue (MB) removal from water	500	O, N	–	Maximum adsorption capacity for methylene blue (MB) (153.37 mg/g)	[80]
Chitosan—Graphene oxide composite aerogel	HTC: 120 °C for 12 h	Adsorption of methyl orange (MO)	–	O, N	297.43	Maximum adsorption capacity high of 48.6 mg/g at PH = 1	[82]
HTC-chitosan carbonaceous material	HTC: 140–220 °C for 10 h	Removal of Cr(VI) from water	60–70 μm	O, N	–	Maximum adsorption capacity for Cr(VI) 388.60 mg/g at 20 °C and pH = 2	[64]
Dual-core Fe_2O_3 @ carbon structure	HTC: 180 °C for 48 h	Removal of Cu ions from water	~500	O, N, Fe	59.60	Maximum adsorption capacity of 104 mg/g for Cr(VI) at 25 °C	[73]
Montmorillonite surface activated with chitosan	HTC: 180 °C and 250 °C for 24 h	Adsorption of polar aflatoxin B ₁ (AFB ₁) and zearalenone (ZER)	200–300	O, N	39.43–180 °C sample 66.15–250 °C sample	The maximum adsorption capacities for AFB ₁ and ZER were 2.05 mg/g and 10.0 mg/g, respectively	[88]
HTC-chitosan carbonaceous adsorbent	HTC: 200 °C 6–48 h	CO ₂ adsorption	–	O, N	1.70–2.60 depending on time	Highest CO ₂ uptake rate of 0.45 mmol/g	[68]
Phosphorylated hydrothermally cross-linked chitosan (HCC-PO ₄)	HTC: 200 °C for 12 h	Uranium removal from wastewater	30–40 μm	O, N, P, U	28.15	Maximum U(VI) adsorption capacity 384.6 mg/g at 298.15 K	[87]
Chitosan@bismuth tungstate coated by silver	HTC: 180 °C for 24 h	Removal of Cu(II) from water	–	O, N, Fe	–	Maximum adsorption capacity was 68.68 mg/g at 25 °C and pH of 6	[86]
Acid-mediated chitosan-based porous carbons	HTC: 200 °C for 5 h	CO ₂ adsorption	–	O, N	263–4168	CO ₂ uptake of 8.36 mmol/g for KOH samples and 7.38 mmol/g for NaOH samples	[74]

Table 2

Studies cover chitosan-sourced carbon materials used for solar cells, batteries, and hydrogen storage applications.

Carbon material type	Preparation condition	Application	Particle size (nm)	Polar groups	S _{BET} (m ² /g)	Results	Ref.
Carbon quantum dots	HTC: 200 °C for 6 h	ZnO nanorods-based nanostructured solar cells	8.1	O, N	–	Light Harvesting Efficiency (LHE): 2% Power Conversion Efficiency (PCE): 0.061%	[93]
Carbon nanodots	HTC: 200 °C for 6 h	TiO ₂ -based nanostructured solar cells	7.91	O, N	–	Light Harvesting Efficiency (LHE): 16.3% Power Conversion Efficiency (PCE): 0.167%	[95]
Carbon quantum dots	HTC: 200 °C for 6 h	Nanostructured solar cells	2–3	O, N	–	Quantum yield: 17.1%	[94]
Hierarchical porous N, O co-doped carbon	HTC: 210 °C for 6 h HTC + KOH: 600 °C for 2 h	Construct carbon/selenium composite cathode for lithium-ion battery	–	O, N, Se	809.30	Discharge capacity of 446.9 mAh g ⁻¹ at rate of 0.24C	[98]
Nitrogen-doped porous carbons	HTC: 220 °C for 12 h HTC + KOH: 600–800 °C for 1 h	Hydrogen storage	–	O, N	1452–2919	Hydrogen storage capacity has changed; from 2.71 wt% at 77 K and 1 bar to 6.77 wt% at 20 bar	[100]

selectivity shifts from Cr(VI) at low pH values (pH = 2–3) to Cu(II) at higher pH readings (pH = 3–5), with the adsorption capacity of 104 mg/g for Cr(VI) at 25 °C. Another magnetic composite called chitosan@ bismuth tungstate coated by silver (MCTS-Ag/Bi₂WO₆) was studied for the same purpose [86]. It resulted in a lower adsorption capacity of Cu (II) compared to Fe₂O₃@carbon microspheres, its maximum adsorption capacity was 68.68 mg/g at room temperature and pH of 6. Moreover, the adsorption process fits the pseudo-second-order kinetic model. In a different study [64], it was found that the maximum adsorption capacity of the HTC-chitosan for Cr(VI) reached 388.60 mg/g at 20 °C and pH = 2. Uranium is another heavy metal successfully removed from wastewater using chitosan based adsorbent [87]. The adsorbent is HTC chitosan crosslinked with phosphate (HCC-PO₄). The theoretical maximum U(VI) adsorption capacity of HCC-PO₄ was 384.6 mg/g at 298.15 K. The adsorbents in previous studies [64,73,86,87] maintained a stable adsorption capacity, as they could be regenerated and reused 5 times.

Adsorption performance is impacted by the surface characteristics of the carbonaceous material [88]. Temperature during the HTC process will impact the produced particles sizes. Higher temperatures lead to smaller particles, and more nitrogen functional groups. This improves the porosity and decreases hydrophobicity of the particles. Wang et al. [88] synthesized montmorillonite functionalized with chitosan and tested it for the adsorption of polar aflatoxin B₁ (AFB₁) and zearalenone (ZER) at 37 °C. The maximum adsorption capacities for AFB₁ and ZER were 2.05 mg/g and 10.0 mg/g, respectively. In addition, the samples prepared with higher HTC temperature showed higher adsorption capacities.

4.1.3. CO₂ capturing

Using chitosan-sourced adsorbents for carbon dioxide (CO₂) capturing has caught the attention of researchers [89]. Its chemical inertness and thermal stability make it suitable for CO₂ adsorption [74]. The mechanism in which chitosan captures the CO₂ molecule is by the formation of ammonium carbamates, which upon heating will dissociate releasing CO₂ gas again [90]. Chitosan based CO₂ adsorbents have 4 times the adsorption capacity of raw chitosan [68]. At 25 °C and 1 bar, the CO₂ uptake rates ranged from 0.1–0.45 mmol/g for chitosan-sourced adsorbents, the adsorbent uptake rate depended on the HTC reaction time needed to prepare it, the longer the time the higher CO₂ uptake rate achieved during the adsorption experiment. The adsorption process followed Freundlich isotherm and the pseudo second-order kinetic model with CO₂ pressure ranging from 0.1–1 Bar. [68]. Kamaran et al. activated the chitosan-sourced carbons with KOH and NaOH for 2 h at 800 °C under a flowing stream of nitrogen. They noticed that would increase the CO₂ uptake to 8.36 mmol/g for KOH samples and 7.38 mmol/g for NaOH sample, the experiment was conducted using Belsorp Max system at 1 bar and 273 K, 283 K, and 298 K [74]. Table 1

summarizes of studies discussing the environmental applications of chitosan-sourced carbon materials.

4.2. Energy applications

4.2.1. Solar cells

Abundant, cheap and non-toxic bio waste such as chitosan have caught the attention of researchers in the energy field; photovoltaics is one of these applications. Semiconductor carbon nanodots exhibit excitation-wavelength-dependent photoluminescence (PL) behavior, making them suitable for applications in the conversion of solar energy [91]. The luminescence properties in carbon dots depend on the composition and the size of the quantum dots [92]. Three different studies have utilized the carbon quantum dots (CQDs) used as sensitizers to build nanostructured solar cells [93]–[95]. Gomes et al. have tested chitosan as precursors to produce semiconductor CQDs. They proved that they are promising for solar energy conversion applications, with quantum yield of 17.1% [94]. Table 2 compares the performance of the different CQDs prepared in these studies.

Briscoe et al. [93] and Marinovic et al. [95] have concluded in their studies that the performance of solar cells depends primarily on the functional groups of the CQDs, functional groups with high nitrogen content show the highest efficiencies.

4.2.2. Batteries

Another application for chitosan-sourced carbonaceous material is in energy storage; more specifically in lithium- selenium (Li–Se) batteries. Building the Se cathode from Se/porous carbon composites can improve the electrochemical conductivity of Se, and improve the utilization efficiency [96,97]. Zhao et al. have used hierarchical porous N, O co-doped carbon material sourced from chitosan to construct carbon/selenium composite cathode as the cathode materials of lithium-ion batteries. This composite delivers a discharge capacity of 446.9 mAh g⁻¹ at rate of 0.24C, while still showing good cycling stability and rate capability. The improved performance is attributed to high specific surface area, and porosity of the prepared hierarchical carbon [98].

4.2.3. Hydrogen storage

The same reasons (high surface area and large microscopic volume) have made carbon materials desirable for hydrogen storage [99]. In a recent study [100], high porosity carbon material prepared by hydrothermal carbonization and chemical activation of chitosan. The HTC process was carried out at 220 °C for 12 h, the resulting highly porous carbons was activated with KOH at temperature between 600 and 800 °C for 1 h. The prepared carbon material was tested for hydrogen storage. By varying the amount of KOH and activation temperature, the nitrogen contents, surface area, and pore volume of the carbon material

Table 3
Comparison between different supercapacitors synthesized from chitosan-sourced carbon materials.

Carbon material type	Preparation condition	Pore size (cm ³ /g)	Polar groups	S _{BET} (m ² /g)	Electrolyte type	Current density (A/g)	Capacitance (F/g)	Capacity retention	Ref.
Nitrogen/sulfur codoped carbon materials	HTC: 200 °C for 12 h HTC further carbonization: 750 °C for 3 h	–	O, N, S	–	6 M KOH	10	135	97.2%	[48]
Hierarchical porous carbon	HTC: 200 °C for 2 h	1.3	O, N	3532	6 M KOH	20	455	99%	[103]
Chitosan-derived carbonaceous materials	HTC: 250 °C for 14 h HTC + KOH: 800 °C for 2 h	1.36	O, N	2200	0.5 M K ₂ SO ₄	0.5	231	–	[104]
					6 M KOH	0.5	305	–	
					0.5 M K ₂ SO ₄	20	154	–	
					6 M KOH	20	198	–	
Nitrogen and phosphorus dual-doped hierarchical porous carbon	HTC: 200 °C for 12 h HTC+ H ₃ PO ₄ : 600–800 °C for 2 h	0.48–0.76 depending on temperature	O, N, P	639–1142 depending on temperature	6 M KOH	0.2	312.4	97%	[107]
					6 M KOH	10	204.4		
Nitrogen and boron codoped activated carbon (BKACS)	HTC: 160 °C for 5 h	2.3658	O, N	1129.60	6 M KOH	0.2	316	–	[49]
					6 M KOH	–	–	96.18%	
Nitrogen-rich hierarchically porous carbon (NHPC)	HTC: 160 °C for 8 h HTC pyrolyzed: 800 °C for 1 h	0.486	O, N, Zn	1067	6 M KOH	1	228.7	98.3%	[110]
						10	–	84.9%	
N-doped porous carbons	HTC: 250 °C for 4 h, 7 h, 10 h and 14 h HTC pyrolyzed: 750 °C for 1 h	0.65–1.25	O, N	1223–2307 depending on time	1.0 M H ₂ SO ₄	0.5	210	91%	[109]
					1.0 M Na ₂ SO ₄	10	191		
					6 M KOH	5 × 10 ^{−3}	223.3	70%	[50]
Nitrogen-doped porous graphene-based aerogels	HTC: 180 °C for 12 h HTC annealed: 900 °C for 2 h	40	O, N	616	6 M KOH	5 × 10 ^{−3}	223.3	70%	[50]
Chitosan-based layered carbon materials	210 °C for 10 h	2.34	O, N	301	1.0 M H ₂ SO ₄	0.2	355	–	[111]
					6 M KOH	0.2	275		

have changed. Therefore, the observed hydrogen storage capacity has changed; it changed from 2.71 wt% at 77 K and 1 bar to 6.77 wt% at 20 bar, it improves with the higher porosity and higher surface area. Table 2 lists chitosan-sourced carbon materials used for solar cells, batteries, and hydrogen storage applications.

4.2.4. Supercapacitors

Supercapacitors are eco-friendly, high-performance, energy-storage and delivery devices. Supercapacitors hold electrical charge either by electrochemical pseudocapacitance or through an electrostatic double-layer mechanism [101]. Supercapacitors' advantages such as the high power delivery, excellent cycle stability and fast charging/discharging

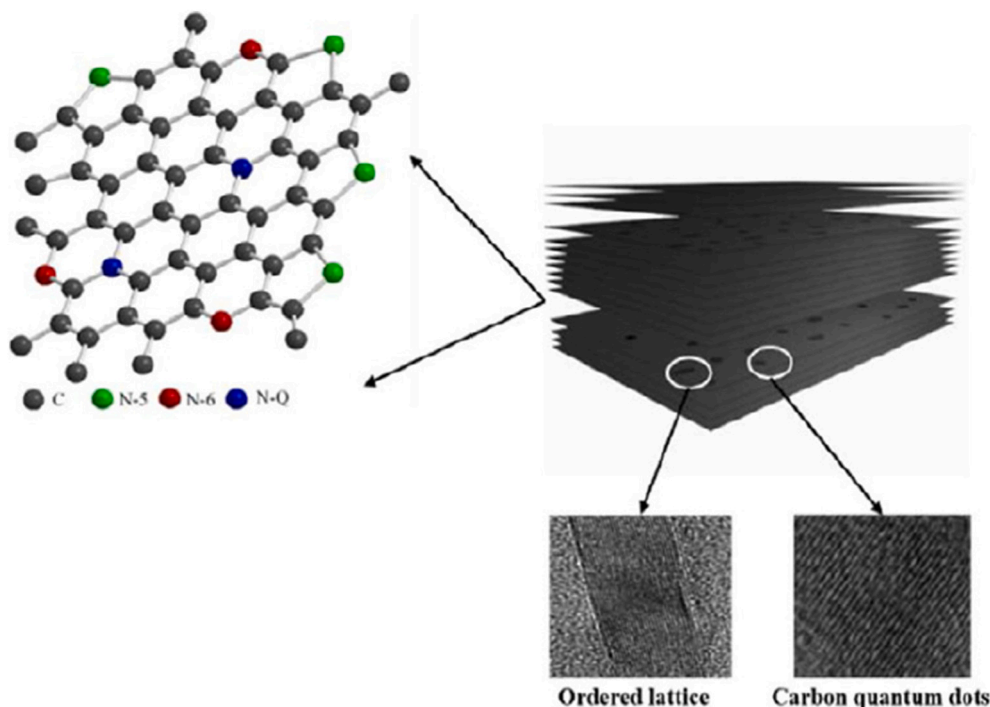


Fig. 8. Structure of fabricated layered porous carbon structure [111].

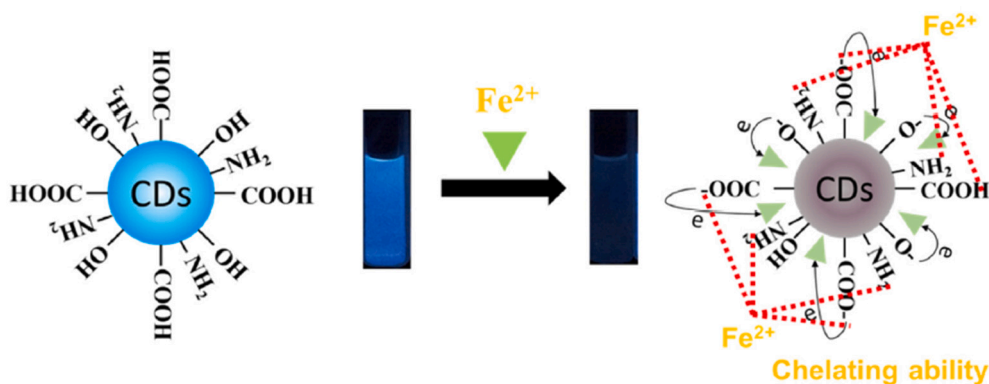


Fig. 9. Detection of ferrous ions based on chelating ability [121].

time [102] have made them attractive to use in portable electronics, energy storage devices and smart grids [103]. Supercapacitors have low energy density compared to batteries [104] which encouraged the researchers to prepare high-performance electrode materials to improve the energy storage capacity [105]. One of the electrode candidate materials is the porous carbons due to their excellent conductivity, favorable stability, abundance and low cost [106]. Many studies aimed at preparing electrical electrodes from chitosan using the HTC process, as summarized in Table 3. It is believed that the high specific surface area, high porosity, and the high nitrogen content of the chitosan-sourced carbonaceous materials improves reduction reactions on the electrode therefore, its performance [104,107].

In one study, the carbon material sourced from chitosan was produced through the HTC process, then activated using acetic acid, to prepare it. Two grams of chitosan was mixed with 55 mL of water, followed by the addition of 15 mL of acetic acid, the obtained viscous solution entered the Teflon lined autoclave, which was operated at 200 °C, and kept for 2 h. This HTC process produced porous carbon with a surface area of 3532 m²/g [108]. Zhu et al. have chosen KOH as an activator for the produced carbonized solids (at 800 °C), which resulted in a specific surface area of 2200 m²/g [104]. A close result (2307 m²/g) was achieved by Tong et al. [109] when they activated their produced carbon with KOH at 750 °C for 1 h, while activating it with KHCO₃ had a slightly lower surface area for nanocarbons (2124 m²/g). Not activating the nanocarbon produced HTC-processed-chitosan will decrease the surface area significantly as seen in (1067 m²/g) [110], and (616 m²/g) [50]. The higher surface area of the carbonaceous material had a positive impact on the electrode capacitance as it could be noticed in Table 3. Wu et al. [111] fabricated a layered porous carbon structure in the presence of an ionic liquid, the chitosan was precursor and was hydrothermally carbonized for 10 h at 210 °C. The produced carbon structure served as nitrogen source and dispersant, it contained many oxygen and nitrogen groups. The maximum capacitance and stability were better in the acidic electrolyte compared to a basic electrolyte as seen in Table 3. Fig. 8 shows the structure of fabricated layered porous carbon structure [111].

Li et al. [48] have codoped the carbon material by nitrogen and sulfur which improved the specific capacitance by almost 100% compared to undoped chitosan. It was also noticed that sulfur is contributing more in improving the capacitance of the carbon. This is explained by the fact that sulfur can lower the internal resistance and improve the conductivity of the carbon materials effectively.

Nitrogen and phosphorus dual-doped porous carbon exhibits excellent electrochemical performance compared to nitrogen-only doped carbon [107]. Moreover, Lin et al. have found that activating carbon with boric acid to produce nitrogen-boron dual-doped carbon would enhance capacitance and the stability of the synthesized electrode. The activation process was done by adding carbon and boric acid in the ratio of 1:2, and followed by placing the mixture into a Teflon-lined

autoclave. The autoclave operated continuously at 160 °C for 5 h [49]. To conclude, activating the carbon material or bi-doping produces a higher surface area electrode leading to better performance and stability. Table 3 compares between different supercapacitors synthesized from chitosan-sourced carbon materials.

4.3. Applications in biosensing and bioelectronics

One of the important processes in environmental monitoring, medicine, biotechnology and industrial process control is electrochemical processes. To overcome the downsides of the traditional electrodes, new materials were developed for electrodes [112]. Among them is carbon nanotubes (CNTs) and Quantum dots (CDQs). This is due to their excellent luminescent properties, high quantum emission efficiencies, high solubility and stability, and low toxicity [113]. For example, Moradi et al. used chitosan as a carbon source to synthesize photoluminescent nano carbon dots [114]. By characterizing the produced nano carbon dots and determining their properties such as dynamic light scattering, and cyclic voltammetry, it was concluded that they are excellent candidates for bio-sensing, biological labeling, medical diagnostics, optoelectronic devices and bio-imaging applications.

Wang et al. synthesized nitrogen-doped carbon nanodots (N-doped CNDs) from chitosan. They reported that the CNDs have excellent quantum yield (31.8%) [115]. This is due to the existence of multiple functional groups (C=O, O—H, COOH, and NH₂) within (N-doped CNDs) [115]. Therefore, they were tested as sensor probes for mercury ions; their detection limit was found to be 80 nM. Furthermore, N-doped CNDs proved to be nontoxic and exhibited excellent biocompatibility when used for live cell imaging.

In the field of electrochemical sensing, (nZrO₂-NH₂C) nanocomposite electrodes [116] and modified carbon quantum dots/multi-wall carbon nanotubes/pencil graphite electrode [117] were used to detect ochratoxin A (OTA) and dextromethorphan (DXM), respectively. In both cases HTC was used to prepare the amino-functionalized nZrO₂-NH₂C nanocomposite, carbon quantum dots (CQDs), and multiwall carbon nanotubes (MWCNT). nZrO₂-NH₂C nanocomposite electrodes were successful in determine OTA with detection range from 1 to 10 ng mL⁻¹ and accuracy of 0.86 μA ng⁻¹ mL cm² at the optimum condition of neutral solution (pH 7) and 30 °C. While the nanotubes/pencil graphite electrode detected the concentration of DXM in the range of 2.0–600 μM, with the detection limit of 0.2 μM.

Some trace elements in the human body are essential for maintaining the function and operation of the organs [118]. Therefore, their deficiencies or overdose may result in various biological disorders and can cause serious harm to the human body. For example, excessive intake of iron ions will result in chronic or acute iron poisoning [119]. While high concentrations of iodine may cause hyperthyroidism [120]. Thus, it is important to develop a simple, cheap and reliable technique for detecting such types of elements in the human body. Carbon dots (CDs)

Table 4

Biosensing, biodetection, and bioelectronics applications of carbonaceous material synthesized from chitosan.

Carbon material type	Preparation condition	Application	Particle size (nm)	Polar groups	Results	Ref.
Carbon quantum dots	HTC: 180 °C for 16 h	Detection of dextromethorphan (DXM)	–	O, N,	The detection range: 2.0–600 μM Detection limit: 0.2 μM	[117]
Nitrogen-doped carbon nanodots	HTC: 220 °C for 12 h	Building sensor probes for mercury ions	3.8	O, N	Detection limit: 80 nM	[115]
Luminescent carbon nano dots	HTC: 250 °C for 45 min	Bioimaging	150	O, N	–	[114]
Zirconia nanoparticles embedded in amino functionalized amorphous carbon (nZrO ₂ -NH ₂ C) nanocomposite	HTC: 180 °C for 18 h	Detection of ochratoxin A (OTA)	–	O, N, Zr	The detection range: 1–10 ng mL ⁻¹ Accuracy: 0.86 $\mu\text{A ng}^{-1}\text{ mL cm}^2$	[116]
Quaternized carbon nanospheres	HTC: 180 °C for 20 h	Antimicrobial activity: killing Gram-positive bacteria	110	O, N	Kill Gram-positive bacteria with dosages: 2.0–5.0 $\mu\text{g mL}^{-1}$	[125]
Carbon quantum dots	HTC: 180 °C for 12 h	Detection of iodine ions	20–30	O, N, Au	Successfully detected I ⁻ ions The detection: 2.3 μM	[122]
Carbon nano dots	HTC: 220 °C for 1 h (microwave)	Detection of Fe ²⁺ ions	–	O, N	The detection range: 0–50 μM Detection limit: 160 nM	[121]

fluorescence prepared from chitosan and acrylamide using microwave-hydrothermal carbonization for the detection of metal ions have been widely reported [121]. The process yield was high and rapid. The presence of amino and carboxylic groups has significantly improved the chelating ability of CDs. Thus, they can detect Fe²⁺ in a concentration range of 0–50 μM and a maximum detection limit of 160 nM. Fig. 9 illustrates the detection process of ferrous ions based on chelating ability [121].

Iodine ions can be detected rapidly using colorimetric methods based on metal nanoparticles such as gold nanoparticles (AuNPs). Song et al. [122] have utilized this technique and prepared carbon quantum dots (CQDs) using chitosan as a precursor. The CQDs were composited with gold nanoparticles using the HTC method. The composite changes color from pink to colorless depending on the amount of I⁻ ions absorbed. The detection limit was estimated to be 2.3 μM indicating high sensitivity and good selectivity toward I⁻.

Since traditional antibiotics are becoming insufficient in defeating bacteria [123]. Nanoparticle (NP)-based antimicrobial strategies have caught the researcher's attention in recent years [124]. NPs special characteristics like high surface energy/surface-to-volume ratio, and abundance of chemical groups on the surface [125]. Jiang et al. [125] have prepared quaternized carbon nanospheres (QCNSs) via a one-step HTC treatment of chitosan and hexadecylbetaine (BS-16). The QCNSs could kill Gram-positive bacteria even at low dosages (of 2.0–5.0 $\mu\text{g mL}^{-1}$), while being intoxic and biocompatible with normal cells and cheap to synthesize. Table 4 lists the biosensing, biodetection, and bioelectronics applications of carbonaceous material synthesized from chitosan.

4.4. Catalysis

Heterogeneous catalysis is one of the hot research topics, and thus new and developed types of catalysts are emerging on a constant basis. Their main advantage is the ease of separating them from the reaction mixture. Thus, they could be easily reused for the following reaction cycles [126]. Among the studied heterogeneous catalysts was the activated carbon as a versatile and green material, characterized by its large specific surface area, high porosity, and the easiness of modifying its surface [127]. Nanostructured carbon materials such as nanotubes are used in a wide field of applications because of their improved electrical and thermal conductivities, as well as low density and high strength [128]. Platinum (Pt)-based electrocatalysts excellent properties are let down by their inactivity due to poisoning [129]. To overcome this issue, new superior support materials are proposed in order to improve the catalyst activity. Among them is titanium dioxide (TiO₂) with its high

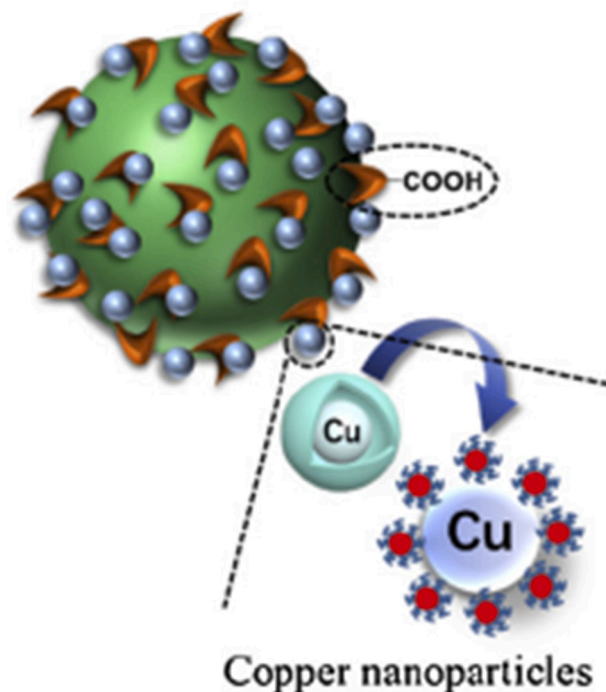


Fig. 10. Illustration of the prepared Cu/hydrochar catalyst for Ullmann C₆N coupling reaction in water [138].

chemical stability under harsh conditions [130]. Therefore, Zhang et al. [131] prepared nitrogen doped chitosan-sourced-carbon coated Mo modified one-dimensional TiO₂ nanowires for methanol electro-oxidation. The mass activity of the prepared catalyst is double the unmodified supported catalyst with 15.9% higher stability. Another approach to overcome (Pt)-based electrocatalysts problems is to design alternative catalysts, such as carbon-based materials (Fe–N–C catalysts) which are particularly promising due to the electrocatalytic and low cost [132,133].

Qiao et al. prepared multiwall carbon nanotubes (MWCNTs) coated with a layer of HTC-nitrogen-doped chitosan [134]. It was used as a catalyst for oxygen reduction reactions. This new catalyst has higher catalytic activity and better resistance for H₂O₂ poisoning. Pirsahab et al. synthesized a chitosan-sourced nano carbon dots (NCDs). The NCDs were prepared using HTC reactions at 180 °C for 2 h. The NCDs

Table 5

Summary of studies discussing the performance of catalysts fabricated from chitosan-sourced carbon materials.

Carbon material type	Preparation condition	Application	Particle size (nm)	Polar groups	S _{BET} (m ² /g)	Results	Ref.
MWCNTs with a layer of biomass derivative N-doped hydrothermal carbons	HTC: 200 °C for 12 h HTC annealed: 1000 °C for 2 h	Catalyst for oxygen reduction reactions	–	O, N, Fe	36–523	High catalytic activity and good resistance for H ₂ O ₂ poisoning	[134]
Bio-polymer based carbon nano dots	HTC: 180 °C for 2 h	Catalyst for H ₂ O ₂ decomposition to remove phenol	65	O, N	–	With H ₂ O ₂ concentration of 12 mmol, 99% phenol was removed in 20 mins	[135]
Nitrogen doped carbon coated Mo modified TiO ₂ nanowires	HTC: 180 °C for 12 h HTC annealed: annealed at 900 °C for 2 h	Catalyst for methanol electrooxidation	1.87–2.62	–	59.7–88.9	Improved the activity of the reaction by 15.9%	[131]
SO ₃ H-functionalized carbonaceous@montmorillonite	HTC: 180 °C for 8 h	Production of bio-lubricant through esterification reaction	200–300	O, N, S	7–164	High activity and yield: 91%	[137]
Hydrochar supported copper nanocatalyst	HTC: 180 °C for 10 h	Catalyst for Ullmann CeN coupling reaction	61.11	O, N	–	High catalytic activity and improved stability	[138]

could catalyze the H₂O₂ decomposition. H₂O₂ dissociates generating free hydroxyl radicals, which in turns oxidized phenol. 99% phenol was removed in just 20 mins at H₂O₂ concentration of 12 mmol and ambient temperature [135].

Solid heterogeneous catalysts could be easily separated from the reaction system which makes them reusable for the next cycle of reactions and “green” [136]. Two such catalysts were prepared through the HTC process; the first is the sulfonated carbonaceous intercalated montmorillonite composite sourced from a mixture of chitosan and furaldehyde [137]. It was used for esterification between trimethylolpropane and oleic acid to produce bio-lubricant. The catalyst composite showed high activity with a yield of 91% in 3 h. The catalytic activity was high after the 5 cycles of reactions. The excellent performance was attributed to the specific high surface area (164.5 m²/g) of the composite. The second heterogeneous catalyst was prepared by Ge et al. [138] in which the fabricated copper nanoparticles were uniformly dispersed on hydrochar. It proved excellent catalytic activity and stability for Ullmann CeN coupling reaction due to its hydrophilicity thus accelerating the coupling reaction in water, Fig. 10 shows the prepared Cu/hydrochar catalyst [138]. Table 5 summarizes the studies discussing the performance of catalysts fabricated from chitosan-sourced carbon materials.

5. Future prospects

While chitosan-based materials proved effective for water treatment applications, it was noticed that most of the conducted tests were on one specific type of contaminants such as methyl orange dye. Thus, it is necessary to study the performance of these adsorbents on a wide range of water pollutants or using real wastewater. It is recommended that the adsorption capacity for heavy metals and CO₂ adsorption and recyclability of these adsorbents be compared to the commercial types.

Functional groups with high nitrogen content resulted in better efficiency-solar-cells. It is recommended to optimize the nitrogen content to improve the solar cell performance. Specific surface area and porosity are the two major factors in carbon material ability to store hydrogen. It would be advisable to synthesize a carbonaceous material with as high as possible porosity and measure its impact on the energy storage. This could be accomplished by raising the reaction temperature during the HTC process. While many studies for supercapacitors were performed, most of them used basic electrolyte despite the fact that the acidic ones might show improved performance. One active field for chitosan-based materials is catalysis. However, the chemical nature of the chitosan-sourced catalysts and its active centers are not fully understood. Therefore, the reaction mechanism is yet to be determined. Knowing this would improve the performance of these catalysts by

modifying their active center, and to develop reaction models. Chitosan as feedstock for carbon material is a promising precursor because of its multiple advantages. Consequently, it is recommended building over the previous studies, and putting more efforts into the development of chitosan-sourced carbon materials.

6. Conclusions

This article reviewed the applications of hydrothermally treated chitosan in the different fields. Furthermore, it discussed HTC process parameters on the properties of the fabricated carbon material and their applications. In the water treatment field, chitosan-sourced adsorbents proved to be successful in adsorbing dyes and heavy metals from wastewater and aqueous solution. In addition, they showed good stability and high recyclability. Chitosan-sourced carbons can capture CO₂ by the formation of ammonium carbamates, which showed high uptake rates for CO₂. Many studies fabricated solar cells by using chitosan as a precursor. Those cells had a relatively high-power conversion efficiency, and high quantum yields. Moreover, chitosan-prepared cathodes discharge capacity of lithium-ion batteries. DXM, mercury ions, OTA, iodine ions, and iron ions, were all successfully detected by probes or sensors fabricated from chitosan. Hence proving the ability of chitosan utilizing in biosensing and bioimaging. Supercapacitors showed wide application for chitosan-sourced carbons. Where in general those supercapacitors had high capacitance, and current densities in different types of electrolytes. Catalysts based on chitosan have been used in many reactions, and showed high catalytic activity and improved stability, while being cheaper to prepare, and more environmentally friendly.

Acknowledgment

Open Access funding provided by the Qatar National Library.

References

- [1] K.H. Adolffson, N. Yadav, M. Hakkarainen, Cellulose-derived hydrothermally carbonized materials and their emerging applications, *Curr. Opin. Green Sustain. Chem.* 23 (2020) 18–24, <https://doi.org/10.1016/j.cogsc.2020.03.008>.
- [2] M. Heidari, A. Dutta, B. Acharya, S. Mahmud, A review of the current knowledge and challenges of hydrothermal carbonization for biomass conversion, *J. Energy Inst.* 92 (6) (2019) 1779–1799, <https://doi.org/10.1016/j.joei.2018.12.003>.
- [3] T. Wang, Y. Zhai, Y. Zhu, C. Li, G. Zeng, A review of the hydrothermal carbonization of biomass waste for hydrochar formation: process conditions, fundamentals, and physicochemical properties, *Renew. Sustain. Energy Rev.* 90 (2018 March) 223–247, <https://doi.org/10.1016/j.rser.2018.03.071>.
- [4] D.P. Yang, Z. Li, M. Liu, X. Zhang, Y. Chen, H. Xue, E. Ye, R. Luque, Biomass-derived carbonaceous materials: recent progress in synthetic approaches,

- advantages, and applications, *ACS Sustain. Chem. Eng.* 7 (5) (2019) 4564–4585, <https://doi.org/10.1021/acssuschemeng.8b06030>.
- [5] R. Antony, T. Arun, S.T.D. Manickam, A review on applications of chitosan-based Schiff bases, *Int. J. Biol. Macromol.* 129 (2019) 615–633, <https://doi.org/10.1016/j.ijbiomac.2019.02.047>.
- [6] F.Sami El-banna, M.E. Mahfouz, S. Loporatti, M. El-Kemary, N.A.N. Hanafy, Chitosan as a natural copolymer with unique properties for the development of hydrogels, *Appl. Sci.* 9 (11) (2019).
- [7] P.K. Dutta, M.N.V. Ravikumar, J. Dutta, Chitin and chitosan for versatile applications, *J. Macromol. Sci. Part C* 42 (3) (Aug. 2002) 307–354, <https://doi.org/10.1081/MC-120006451>.
- [8] V. Zargar, M. Asghari, A. Dashti, A review on chitin and chitosan polymers: structure, chemistry, solubility, derivatives, and applications, *ChemBioEng Rev.* 2 (3) (2015) 204–226, <https://doi.org/10.1002/cben.201400025>.
- [9] M.N.V. Ravi Kumar, A review of chitin and chitosan applications, *React. Funct. Polym.* 46 (1) (2000) 1–27, [https://doi.org/10.1016/S1381-5148\(00\)00038-9](https://doi.org/10.1016/S1381-5148(00)00038-9).
- [10] E.-J. Lee, D.-S. Shin, H.-E. Kim, H.-W. Kim, Y.-H. Koh, J.-H. Jang, Membrane of hybrid chitosan-silica xerogel for guided bone regeneration, *Biomaterials* 30 (5) (Feb. 2009) 743–750, <https://doi.org/10.1016/j.biomaterials.2008.10.025>.
- [11] H. Nagahama, N. Nwe, R. Jayakumar, S. Koiwa, T. Furuike, H. Tamura, Novel biodegradable chitin membranes for tissue engineering applications, *Carbohydr. Polym.* 73 (2) (2008) 295–302, <https://doi.org/10.1016/j.carbpol.2007.11.034>.
- [12] K. Madhumathi, N.S. Binulal, H. Nagahama, H. Tamura, K.T. Shalumon, N. Selvamurugan, S.V. Nair, R. Jayakumar, Preparation and characterization of novel β -chitin-hydroxyapatite composite membranes for tissue engineering applications, *Int. J. Biol. Macromol.* 44 (1) (2009) 1–5, <https://doi.org/10.1016/j.ijbiomac.2008.09.013>.
- [13] Y.L. Nunes, F.L. de Menezes, I.G. de Sousa, A.L.G. Cavalcante, F.T.T. Cavalcante, K. da Silva Moreira, A.L.B. de Oliveira, G.F. Mota, J.E. da Silva Souza, I.R. de Aguiar Falcão, T.G. Rocha, R.B.R. Valério, P.B.A. Fachine, M.C.M. de Souza, J.C. S. dos Santos, Chemical and physical Chitosan modification for designing enzymatic industrial biocatalysts: how to choose the best strategy? *Int. J. Biol. Macromol.* 181 (2021) 1124–1170, <https://doi.org/10.1016/j.ijbiomac.2021.04.004>.
- [14] S. Moalla, I. Ammar, M.L. Fauconnier, S. Danthine, C. Blecker, S. Besbes, H. Attia, Development and characterization of chitosan films carrying *Artemisia campestris* antioxidants for potential use as active food packaging materials, *Int. J. Biol. Macromol.* 183 (2021) 254–266, <https://doi.org/10.1016/j.ijbiomac.2021.04.113>.
- [15] W. Liu, M. Zhang, A.S. Mujumdar, B. Chitrakar, D. Yu, Effects of chitosan coating on freeze-drying of blueberry enhanced by ultrasound pre-treatment in sodium bicarbonate medium, *Int. J. Biol. Macromol.* 181 (2021) 631–643, <https://doi.org/10.1016/j.ijbiomac.2021.03.172>.
- [16] K.R. Shouair, N. El-Desouky, M.M. Rashad, M.K. Ahmed, I. Janowska, M. El-Kemary, Chitosan based-nanoparticles and nanocapsules: Overview, physicochemical features, applications of a nanofibrous scaffold, and bioprinting, *Int. J. Biol. Macromol.* 167 (2021) 1176–1197, <https://doi.org/10.1016/j.ijbiomac.2020.11.072>.
- [17] A. Salama, Recent progress in preparation and applications of chitosan/calcium phosphate composite materials, *Int. J. Biol. Macromol.* 178 (2021) 240–252, <https://doi.org/10.1016/j.ijbiomac.2021.02.143>.
- [18] P. Maleki Dana, J. Hallajzadeh, Z. Asemi, M.A. Mansournia, B. Yousefi, Chitosan applications in studying and managing osteosarcoma, *Int. J. Biol. Macromol.* 169 (2021) 321–329, <https://doi.org/10.1016/j.ijbiomac.2020.12.058>.
- [19] H.B. Quesada, T.P. de Araújo, D.T. Vareschini, M.A.S.D. de Barros, R.G. Gomes, R. Bergamasco, Chitosan, alginate and other macromolecules as activated carbon immobilizing agents: a review on composite adsorbents for the removal of water contaminants, *Int. J. Biol. Macromol.* 164 (2020) 2535–2549, <https://doi.org/10.1016/j.ijbiomac.2020.08.118>.
- [20] N.S. Abdul Mubarak, N.N. Bahrudin, A.H. Jawad, B.H. Hameed, S. Sabar, Microwave enhanced synthesis of sulfonated chitosan-montmorillonite for effective removal of methylene blue, *J. Polym. Environ.* (2021), <https://doi.org/10.1007/s10924-021-02172-9>.
- [21] Annu, A.N. Raja, Recent development in chitosan-based electrochemical sensors and its sensing application, *Int. J. Biol. Macromol.* 164 (2020) 4231–4244, <https://doi.org/10.1016/j.ijbiomac.2020.09.012>.
- [22] G. Malucelli, Flame-retardant systems based on chitosan and its derivatives: state of the art and perspectives, *Molecules* 25 (18) (2020), <https://doi.org/10.3390/molecules25184046>.
- [23] N. Hammi, S. Chen, F. Dumeignil, S. Royer, A. El Kadib, Chitosan as a sustainable precursor for nitrogen-containing carbon nanomaterials: synthesis and uses, *Mater. Today Sustain.* 10 (2020) 100053, <https://doi.org/10.1016/j.mtsust.2020.100053>.
- [24] Z. Li, R.A.B. Rosli, Y. Xiang, E. Ye, X.J. Loh, Carbon precursor from lignin: methods and applications, in: *Functional Materials From Lignin 3*, World Scientific, Europe, 2017, pp. 121–152, https://doi.org/10.1142/9781786345219_0005.
- [25] S. Nizamuddin, A. Jadhav, S.S. Qureshi, H.A. Baloch, M.T.H. Siddiqui, N. M. Mubarak, G. Griffin, S. Madapusi, A. Tanksale, M.I. Ahamed, Synthesis and characterization of polylactide/rice husk hydrochar composite, *Sci. Rep.* 9 (1) (2019) 5445, <https://doi.org/10.1038/s41598-019-41960-1>.
- [26] H. Gao, C.P. Teng, D. Huang, W. Xu, C. Zheng, Y. Chen, M. Liu, D.-P. Yang, M. Lin, Z. Li, E. Ye, Microwave assisted synthesis of luminescent carbonaceous nanoparticles from silk fibroin for bioimaging, *Mater. Sci. Eng. C* 80 (2017) 616–623, <https://doi.org/10.1016/j.msec.2017.07.007>.
- [27] W.S. Wan Ngah, L.C. Teong, M.A.K.M. Hanafiah, Adsorption of dyes and heavy metal ions by chitosan composites: a review, *Carbohydr. Polym.* 83 (4) (2011) 1446–1456, <https://doi.org/10.1016/j.carbpol.2010.11.004>.
- [28] R. Sharma, K. Jasrotia, N. Singh, P. Ghosh, S. Srivastava, N.R. Sharma, J. Singh, R. Kanwar, A. Kumar, A comprehensive review on hydrothermal carbonization of biomass and its applications, *Chem. Africa* 3 (2020) 1–19, <https://doi.org/10.1007/s42250-019-00098-3>.
- [29] M.J. Ahmed, B.H. Hameed, E.H. Hummadi, Review on recent progress in chitosan/chitin-carbonaceous material composites for the adsorption of water pollutants, *Carbohydr. Polym.* vol. 247, no. February (2020) 116690, <https://doi.org/10.1016/j.carbpol.2020.116690>.
- [30] S.H. Rimu, M.M. Rahman, Insight of chitosan-based nanocomposite for removal of hexavalent chromium from wastewater- a review, *Int. J. Environ. Anal. Chem.* (Sep. 2020) 1–18, <https://doi.org/10.1080/03067319.2020.1817426>.
- [31] R.S. Varma, in: *Biomass-derived Renewable Carbonaceous Materials for Sustainable Chemical and Environmental Applications* 7, 2019, pp. 6458–6470, <https://doi.org/10.1021/acssuschemeng.8b06550>.
- [32] V.F. Lee, *Solution and Shear Properties of Chitin and Chitosan*, University of Washington, 1974 [Online]. Available: <https://books.google.com.qa/books?id=6HAXtwAACAAJ>.
- [33] V.K. Thakur, M.K. Thakur, Recent advances in graft copolymerization and applications of chitosan: a review, *ACS Sustain. Chem. Eng.* 2 (12) (2014) 2637–2652, <https://doi.org/10.1021/sc500634p>.
- [34] D. Liu, Y. Zhu, Z. Li, M. Xiao, C. Jiang, M. Chen, Y. Chen, Microfibrillar polysaccharide-derived biochars as sodium benzoate adsorbents, *ACS Omega* 2 (6) (Jun. 2017) 2959–2966, <https://doi.org/10.1021/acsomega.7b00404>.
- [35] H.S. Kambo, A. Dutta, A comparative review of biochar and hydrochar in terms of production, physico-chemical properties and applications, *Renew. Sust. Energ. Rev.* 45 (2015) 359–378, <https://doi.org/10.1016/j.rser.2015.01.050>.
- [36] J. Mumme, L. Eckervogt, J. Pielert, M. Diakité, F. Rupp, J. Kern, Hydrothermal carbonization of anaerobically digested maize silage, *Bioresour. Technol.* 102 (19) (2011) 9255–9260, <https://doi.org/10.1016/j.biortech.2011.06.099>.
- [37] J.A. Libra, K.S. Ro, C. Kammann, A. Funke, N.D. Berge, Y. Neubauer, M. M. Titrici, C. Fühner, O. Bens, J. Kern, K.H. Emmerich, Hydrothermal carbonization of biomass residuals: a comparative review of the chemistry, processes and applications of wet and dry pyrolysis, *Biofuels* 2 (1) (2011) 71–106, <https://doi.org/10.4155/bfs.10.81>.
- [38] A. Funke, F. Ziegler, Hydrothermal carbonization of biomass: a summary and discussion of chemical mechanisms for process engineering, *Biofuels Bioprod. Biorefining* 4 (2) (Mar. 2010) 160–177, <https://doi.org/10.1002/bbb.198>.
- [39] K. Ghosal, A. Ghosh, Carbon dots: the next generation platform for biomedical applications, *Mater. Sci. Eng. C* 96 (2019) 887–903, <https://doi.org/10.1016/j.msec.2018.11.060>.
- [40] A. Sharma, J. Das, Small molecules derived carbon dots: synthesis and applications in sensing, catalysis, imaging, and biomedicine, *J. Nanobiotechnology* 17 (1) (2019) 92, <https://doi.org/10.1186/s12951-019-0525-8>.
- [41] M. Han, S. Zhu, S. Lu, Y. Song, T. Feng, S. Tao, J. Liu, B. Yang, Recent progress on the photocatalysis of carbon dots: classification, mechanism and applications, *Nano Today* 19 (2018) 201–218, <https://doi.org/10.1016/j.nantod.2018.02.008>.
- [42] M.L. Liu, B. Bin Chen, C.M. Li, C.Z. Huang, Carbon dots: synthesis formation mechanism fluorescence origin and sensing applications, *Green Chem.* 21 (3) (2019) 449–471, <https://doi.org/10.1039/C8GC02736F>.
- [43] C. Xia, S. Zhu, T. Feng, M. Yang, B. Yang, Evolution and synthesis of carbon dots: from carbon dots to carbonized polymer dots, *Adv. Sci.* 6 (23) (Dec. 2019) 1901316, <https://doi.org/10.1002/adv.201901316>.
- [44] X. Miao, D. Qu, D. Yang, B. Nie, Y. Zhao, H. Fan, Z. Sun, Synthesis of carbon dots with multiple color emission by controlled graphitization and surface functionalization, *Adv. Mater.* 30 (1) (Jan. 2018) 1704740, <https://doi.org/10.1002/adma.201704740>.
- [45] T. Feng, Q. Zeng, S. Lu, X. Yan, J. Liu, S. Tao, M. Yang, B. Yang, Color-tunable carbon dots possessing solid-state emission for full-color light-emitting diodes applications, *ACS Photonics* 5 (2) (Feb. 2018) 502–510, <https://doi.org/10.1021/acsp Photonics.7b01010>.
- [46] C. Liu, F. Zhang, J. Hu, W. Gao, M. Zhang, A mini review on pH-sensitive photoluminescence in carbon nanodots, *Front. Chem.* 8 (2021) 1242, <https://doi.org/10.3389/fchem.2020.605028>.
- [47] Q. Zhou, Q. Gao, W. Luo, C. Yan, Z. Ji, P. Duan, One-step synthesis of amino-functionalized attapulgite clay nanoparticles adsorbent by hydrothermal carbonization of chitosan for removal of methylene blue from wastewater, *Colloids Surf. A Physicochem. Eng. Asp.* 470 (2015) 248–257, <https://doi.org/10.1016/j.colsurfa.2015.01.092>.
- [48] M. Li, X. Han, X. Chang, W. Yin, J. Ma, Nitrogen/sulfur-codoped carbon materials from chitosan for supercapacitors, *J. Electron. Mater.* 45 (8) (2016) 4331–4337, <https://doi.org/10.1007/s11664-016-4644-9>.
- [49] Z. Lin, X. Xiang, S. Peng, X. Jiang, L. Hou, Facile synthesis of chitosan-based carbon with rich porous structure for supercapacitor with enhanced electrochemical performance, *J. Electroanal. Chem.* 823 (2018) 563–572, <https://doi.org/10.1016/j.jelechem.2018.06.031>.
- [50] Z. Xie, J. Zhu, Y. Bi, H. Ren, X. Chen, H. Yu, Nitrogen-Doped porous graphene-based aerogels toward efficient heavy metal ion adsorption and supercapacitor applications, *Phys. Status Solidi Rapid Res. Lett.* 14 (1) (2020) 1–8, <https://doi.org/10.1002/psrr.201900534>.
- [51] Y. Sun, B. Gao, Y. Yao, J. Fang, M. Zhang, Y. Zhou, H. Chen, L. Yang, Effects of feedstock type, production method, and pyrolysis temperature on biochar and

- hydrochar properties, *Chem. Eng. J.* 240 (2014) 574–578, <https://doi.org/10.1016/j.cej.2013.10.081>.
- [52] X. Cao, K.S. Ro, J.A. Libra, C.I. Kammann, I. Lima, N. Berge, L. Li, Y. Li, N. Chen, J. Yang, B. Deng, J. Mao, Effects of Biomass Types and Carbonization Conditions on the Chemical Characteristics of Hydrochars, *J. Agric. Food Chem.* 61 (39) (Oct. 2013) 9401–9411, <https://doi.org/10.1021/jf402345k>.
- [53] M.-M. Titirici, M. Antonietti, Chemistry and materials options of sustainable carbon materials made by hydrothermal carbonization, *Chem. Soc. Rev.* 39 (1) (2010) 103–116, <https://doi.org/10.1039/B819318P>.
- [54] M.-M. Titirici, A. Thomas, M. Antonietti, Back in the black: hydrothermal carbonization of plant material as an efficient chemical process to treat the CO₂ problem? *New J. Chem.* 31 (6) (2007) 787–789, <https://doi.org/10.1039/B616045J>.
- [55] Y. Shen, A review on hydrothermal carbonization of biomass and plastic wastes to energy products, *Biomass Bioenergy* 134 (August 2019) (2020) 105479, <https://doi.org/10.1016/j.biombioe.2020.105479>.
- [56] D. Ma, Q. Feng, B. Chen, X. Cheng, K. Chen, J. Li, Insight into chlorine evolution during hydrothermal carbonization of medical waste model, *J. Hazard. Mater.* 380 (2019), 120847, <https://doi.org/10.1016/j.jhazmat.2019.120847>.
- [57] H.B. Sharma, A.K. Sarmah, B. Dubey, Hydrothermal carbonization of renewable waste biomass for solid biofuel production: a discussion on process mechanism, the influence of process parameters, environmental performance and fuel properties of hydrochar, *Renew. Sust. Energ. Rev.* vol. 123, no. February (2020) 109761, <https://doi.org/10.1016/j.rser.2020.109761>.
- [58] S. Nizamuddin, H.A. Baloch, M.T.H. Siddiqui, N.M. Mubarak, M.M. Tunio, A. W. Bhutto, A.S. Jatoti, G.J. Griffin, M.P. Srinivasan, An overview of microwave hydrothermal carbonization and microwave pyrolysis of biomass, *Rev. Environ. Sci. Biotechnol.* 17 (4) (2018) 813–837, <https://doi.org/10.1007/s11157-018-9476-z>.
- [59] M. Guiotoku, C.R. Rambo, D. Hotza, Charcoal produced from cellulosic raw materials by microwave-assisted hydrothermal carbonization, *J. Therm. Anal. Calorim.* 117 (1) (2014) 269–275, <https://doi.org/10.1007/s10973-014-3676-8>.
- [60] M. Bhattacharya, T. Basak, A review on the susceptor assisted microwave processing of materials, *Energy* 97 (2016) 306–338, <https://doi.org/10.1016/j.energy.2015.11.034>.
- [61] Z. Feng, A. Simeone, K. Odelius, M. Hakkarainen, Biobased nanographene oxide creates stronger chitosan hydrogels with improved adsorption capacity for trace pharmaceuticals, *ACS Sustain. Chem. Eng.* 5 (12) (2017) 11525–11535, <https://doi.org/10.1021/acsschemeng.7b02809>.
- [62] M. Guiotoku, in: C. Rambo (Ed.), *Synthesis of Carbon-based Materials by Microwave-assisted Hydrothermal Process*, IntechOpen, Rijeka, 2011, <https://doi.org/10.5772/20089>. Ch. 13.
- [63] S. Jia, S. Jia, S. Jia, H. Pan, H. Pan, H. Pan, Q. Lin, Q. Lin, X. Wang, X. Wang, C. Li, C. Li, M. Wang, Y. Shi, Y. Shi, Study on the preparation and mechanism of chitosan-based nano-mesoporous carbons by hydrothermal method, *Nanotechnology* 31 (36) (2020) 365604, <https://doi.org/10.1088/1361-6528/ab9575>.
- [64] F. Shen, J. Su, X. Zhang, K. Zhang, X. Qi, Chitosan-derived carbonaceous material for highly efficient adsorption of chromium (VI) from aqueous solution, *Int. J. Biol. Macromol.* vol. 91, no. Vi (2016) 443–449, <https://doi.org/10.1016/j.ijbiomac.2016.05.103>.
- [65] A.J. Ramiro de Castro, G.D. Saraiva, A.C. Oliveira, V.O. Sousa Neto, A.J. Paula, A. G. Souza Filho, O.P. Ferreira, Ordered porous carbons from hydrothermally treated biomass: effects of the thermal treatments on the structure and porosity, *Vib. Spectrosc.* 111 (2020) 103175, <https://doi.org/10.1016/j.vibspec.2020.103175>.
- [66] K. Nakason, B. Panyapinyopol, V. Kanokkantaopong, N. Viriya-empikul, W. Kraithong, P. Pavasant, Hydrothermal carbonization of unwanted biomass materials: effect of process temperature and retention time on hydrochar and liquid fraction, *J. Energy Inst.* 91 (5) (2018) 786–796, <https://doi.org/10.1016/j.joei.2017.05.002>.
- [67] H. Simsir, N. Eltugral, S. Karagoz, Hydrothermal carbonization for the preparation of hydrochars from glucose, cellulose, chitin, chitosan and wood chips via low-temperature and their characterization, *Bioresour. Technol.* 246 (2017) 82–87, <https://doi.org/10.1016/j.biortech.2017.07.018>.
- [68] J.A.O. Chagas, G.O. Crispim, B.P. Pinto, R.A.S.S. Gil, C.J.A. Mota, Synthesis, characterization, and CO₂ uptake of adsorbents prepared by hydrothermal carbonization of chitosan, *ACS Omega* 5 (45) (2020) 29520–29529, <https://doi.org/10.1021/acsomega.0c04470>.
- [69] C. Leginhas, J.M.V. Nabais, M.M. Titirici, Activated carbons with high nitrogen content by a combination of hydrothermal carbonization with activation, *Microporous Mesoporous Mater.* 226 (2016) 125–132, <https://doi.org/10.1016/j.micromeso.2015.12.047>.
- [70] M. Sevilla, J.A. Maciá-Agulló, A.B. Fuentes, Hydrothermal carbonization of biomass as a route for the sequestration of CO₂: chemical and structural properties of the carbonized products, *Biomass Bioenergy* 35 (7) (2011) 3152–3159, <https://doi.org/10.1016/j.biombioe.2011.04.032>.
- [71] S. Román, J.M. Valente Nabais, B. Ledesma, J.F. González, C. Leginhas, M. M. Titirici, Production of low-cost adsorbents with tunable surface chemistry by conjunction of hydrothermal carbonization and activation processes, *Microporous Mesoporous Mater.* 165 (2013) 127–133, <https://doi.org/10.1016/j.micromeso.2012.08.006>.
- [72] B. Zhang, Y. Huayan, J. Wang, X. Chen, H. Zhang, Q. Zhang, Fe3O4@SiO2@CCS porous magnetic microspheres as adsorbent for removal of organic dyes in aqueous phase, *J. Alloys Compd.* 735 (2018) 1986–1996, <https://doi.org/10.1016/j.jallcom.2017.11.349>.
- [73] X. Wang, C. Zhan, Y. Ding, B. Ding, Y. Xu, S. Liu, H. Dong, Dual-core Fe2O3@Carbon structure derived from hydrothermal carbonization of chitosan as a highly efficient material for selective adsorption, *ACS Sustain. Chem. Eng.* 5 (2) (2017) 1457–1467, <https://doi.org/10.1021/acssuschemeng.6b02034>.
- [74] U. Kamran, S.J. Park, Tuning ratios of KOH and NaOH on acetic acid-mediated chitosan-based porous carbons for improving their textural features and CO₂ uptakes, *J. CO₂ Util.* vol. 40, no. April (2020) 101212, <https://doi.org/10.1016/j.jcou.2020.101212>.
- [75] Z. Zhang, Z. Zhang, Y. Fernández, J.A. Menéndez, H. Niu, J. Peng, L. Zhang, S. Guo, Adsorption isotherms and kinetics of methylene blue on a low-cost adsorbent recovered from a spent catalyst of vinyl acetate synthesis, *Appl. Surf. Sci.* 256 (8) (2010) 2569–2576, <https://doi.org/10.1016/j.apsusc.2009.10.106>.
- [76] F. Delval, G. Crini, N. Morin, J. Vebrel, S. Bertini, G. Torri, The sorption of several types of dye on crosslinked polysaccharides derivatives, *Dyes Pigments* 53 (1) (2002) 79–92, [https://doi.org/10.1016/S0143-7208\(02\)00004-9](https://doi.org/10.1016/S0143-7208(02)00004-9).
- [77] M. Rafatullah, O. Sulaiman, R. Hashim, A. Ahmad, Adsorption of methylene blue on low-cost adsorbents: a review, *J. Hazard. Mater.* 177 (1) (2010) 70–80, <https://doi.org/10.1016/j.jhazmat.2009.12.047>.
- [78] F. Marrakchi, B.H. Hameed, E.H. Hummadi, Mesoporous biohybrid epichlorohydrin crosslinked chitosan/carbon-clay adsorbent for effective cationic and anionic dyes adsorption, *Int. J. Biol. Macromol.* 163 (2020) 1079–1086, <https://doi.org/10.1016/j.ijbiomac.2020.07.032>.
- [79] N.H. Yusof, K.Y. Foo, B.H. Hameed, M.H. Hussin, H.K. Lee, S. Sabar, One-step synthesis of chitosan-polyethyleneimine with calcium chloride as effective adsorbent for Acid Red 88 removal, *Int. J. Biol. Macromol.* 157 (2020) 648–658, <https://doi.org/10.1016/j.ijbiomac.2019.11.218>.
- [80] X. Zhao, X. Ma, P. Zheng, The preparation of carboxylic-functional carbon-based nanofibers for the removal of cationic pollutants, *Chemosphere* 202 (2018) 298–305, <https://doi.org/10.1016/j.chemosphere.2018.03.131>.
- [81] C. He, H. Lin, L. Dai, R. Qiu, Y. Tang, Y. Wang, P.G. Duan, Y.S. Ok, Waste shrimp shell-derived hydrochar as an emergent material for methyl orange removal in aqueous solutions, *Environ. Int.* 134 (September 2019) (2020) 105340, <https://doi.org/10.1016/j.envint.2019.105340>.
- [82] W. Zhu, X. Jiang, F. Liu, F. You, C. Yao, Preparation of chitosan — graphene oxide composite aerogel by hydrothermal method and its adsorption property of methyl orange, *Polym.* 12 (9) (2020) 2169, <https://doi.org/10.3390/polym12092169>. PMID: 32972013; PMCID: PMC7570273.
- [83] K. Jomova, M. Valko, Advances in metal-induced oxidative stress and human disease, *Toxicology* 283 (2) (2011) 65–87, <https://doi.org/10.1016/j.toxic.2011.03.001>.
- [84] M. Monier, D.M. Ayad, Y. Wei, A.A. Sarhan, Adsorption of Cu(II), Co(II), and Ni (II) ions by modified magnetic chitosan chelating resin, *J. Hazard. Mater.* 177 (1) (2010) 962–970, <https://doi.org/10.1016/j.jhazmat.2010.01.012>.
- [85] X. Wang, J. Liu, W. Xu, One-step hydrothermal preparation of amino-functionalized carbon spheres at low temperature and their enhanced adsorption performance towards Cr(VI) for water purification, *Colloids Surf. A Physicochem. Eng. Asp.* 415 (2012) 288–294, <https://doi.org/10.1016/j.colsurfa.2012.09.035>.
- [86] L. Yang, Y. Peng, C. Qian, G. Xing, J. He, C. Zhao, B. Lai, Enhanced adsorption / photocatalytic removal of Cu (II) from wastewater by a novel magnetic chitosan @ bismuth tungstate coated by silver (MCTS-Ag / Bi₂WO₆) composite, *Chemosphere* 263 (2021), 128120, <https://doi.org/10.1016/j.chemosphere.2020.128120>.
- [87] Y. Sun, Y. Kang, W. Zhong, Y. Liu, Y. Dai, A simple phosphorylation modification of hydrothermally cross-linked chitosan for selective and efficient removal of U (VI), *J. Solid State Chem.* 292 (2020) 121731, <https://doi.org/10.1016/j.jssc.2020.121731>.
- [88] G. Wang, J. Xu, Z. Sun, S. Zheng, Surface functionalization of montmorillonite with chitosan and the role of surface properties on its adsorptive performance: a comparative study on mycotoxins adsorption, *Langmuir* 36 (10) (2020) 2601–2611, <https://doi.org/10.1021/acslangmuir.9b03673>.
- [89] M. Azharul Islam, Y.L. Tan, M. Atikul Islam, M. Romic, B.H. Hameed, Chitosan-bleaching earth clay composite as an efficient adsorbent for carbon dioxide adsorption: process optimization, *Colloids Surf. A Physicochem. Eng. Asp.* 554 (2018) 9–15, <https://doi.org/10.1016/j.colsurfa.2018.06.021>.
- [90] M.L. Pinto, L. Mafra, J.M. Guil, J. Pires, J. Rocha, Adsorption and Activation of CO₂ by Amine-Modified Nanoporous Materials Studied by Solid-State NMR and ¹³CO₂ Adsorption, *Chem. Mater.* 23 (6) (Mar. 2011) 1387–1395, <https://doi.org/10.1021/cm1029563>.
- [91] C. Doñate-Buendia, R. Torres-Mendieta, A. Pyatenko, E. Falomir, M. Fernández-Alonso, G. Mínguez-Vega, Fabrication by laser irradiation in a continuous flow jet of carbon quantum dots for fluorescence imaging, *ACS Omega* 3 (3) (Mar. 2018) 2735–2742, <https://doi.org/10.1021/acsomega.7b02082>.
- [92] H. M. R. G. J.C.G.E. da Silva, A new insight on silicon dots, *Curr. Anal. Chem.* 8 (1) (2012) 67–77, <https://doi.org/10.2174/157341112798472260>.
- [93] J. Briscoe, A. Marinovic, M. Sevilla, S. Dunn, M. Titirici, Biomass-derived carbon quantum dot sensitizers for solid-state nanostructured solar cells, *Angew. Chemie - Int. Ed.* 54 (15) (2015) 4463–4468, <https://doi.org/10.1002/anie.201409290>.
- [94] M.F. Gomes, Y.F. Gomes, A. Lopes-Moriyama, E.L. de Barros Neto, C.P. de Souza, Design of carbon quantum dots via hydrothermal carbonization synthesis from renewable precursors, *Biomass Convers. Biorefinery* 9 (4) (2019) 689–694, <https://doi.org/10.1007/s13399-019-00387-4>.
- [95] A. Marinovic, L.S. Kiat, S. Dunn, M.M. Titirici, J. Briscoe, Carbon-nanodot solar cells from renewable precursors, *ChemSusChem* 10 (5) (2017) 1004–1013, <https://doi.org/10.1002/cssc.201601741>.

- [96] M.-N. Liu Wan-Fei Li Jian Wang, Yue-Gang Zhang Progress of lithium/sulfur batteries based on chemically modified carbon Acta Phys.-Chim. Sin. 33 1 165 182 <http://www.whxb.pku.edu.cn>.
- [97] X. Wang, Z. Zhang, Y. Qu, G. Wang, Y. Lai, J. Li, Solution-based synthesis of multi-walled carbon nanotube/selenium composites for high performance lithium–selenium battery, *J. Power Sources* 287 (2015) 247–252, <https://doi.org/10.1016/j.jpowsour.2015.04.052>.
- [98] C. Zhao, J. Luo, Z. Hu, Hierarchical porous n, O Co-doped carbon/Se composite derived from hydrothermal treated chitosan as li–Se battery cathode, *Micro Nano Lett.* 13 (10) (2018) 1386–1389, <https://doi.org/10.1049/mnl.2018.5154>.
- [99] Z. Yang, Y. Xia, R. Mokaya, Enhanced hydrogen storage capacity of high surface area zeolite-like carbon materials, *J. Am. Chem. Soc.* 129 (6) (Feb. 2007) 1673–1679, <https://doi.org/10.1021/ja067149g>.
- [100] Z. Wang, L. Sun, F. Xu, H. Zhou, X. Peng, D. Sun, J. Wang, Y. Du, Nitrogen-doped porous carbons with high performance for hydrogen storage, *Int. J. Hydrog. Energy* 41 (20) (2016) 8489–8497, <https://doi.org/10.1016/j.ijhydene.2016.03.023>.
- [101] S. Gao, K. Geng, H. Liu, X. Wei, M. Zhang, P. Wang, J. Wang, Transforming organic-rich amaranthus waste into nitrogen-doped carbon with superior performance of the oxygen reduction reaction, *Energy Environ. Sci.* 8 (1) (2015) 221–229, <https://doi.org/10.1039/C4EE02087A>.
- [102] Z. Chen, X. Peng, X. Zhang, S. Jing, L. Zhong, R. Sun, Facile synthesis of cellulose-based carbon with tunable N content for potential supercapacitor application, *Carbohydr. Polym.* 170 (2017) 107–116, <https://doi.org/10.1016/j.carbpol.2017.04.063>.
- [103] L. Xie, G. Sun, F. Su, X. Guo, Q. Kong, X. Li, X. Huang, L. Wan, W. Song, K. Li, C. Lv, C.-M. Chen, Hierarchical porous carbon microtubes derived from willow catkins for supercapacitor applications, *J. Mater. Chem. A* 4 (5) (2016) 1637–1646, <https://doi.org/10.1039/C5TA09043A>.
- [104] L. Zhu, F. Shen, R.L. Smith, X. Qi, High-Performance supercapacitor electrode materials from chitosan via hydrothermal carbonization and potassium hydroxide activation, *Energy Technol.* 5 (3) (2017) 452–460, <https://doi.org/10.1002/ente.201600337>.
- [105] J. Wang, P. Nie, B. Ding, S. Dong, X. Hao, H. Dou, X. Zhang, Biomass derived carbon for energy storage devices, *J. Mater. Chem. A* 5 (6) (2017) 2411–2428, <https://doi.org/10.1039/C6TA08742F>.
- [106] X. He, N. Zhang, X. Shao, M. Wu, M. Yu, J. Qiu, A layered-template-nanospace-confinement strategy for production of corrugated graphene nanosheets from petroleum pitch for supercapacitors, *Chem. Eng. J.* 297 (2016) 121–127, <https://doi.org/10.1016/j.cej.2016.03.153>.
- [107] X. Zhao, S. Wang, Q. Wu, Nitrogen and phosphorus dual-doped hierarchical porous carbon with excellent supercapacitance performance, *Electrochim. Acta* 247 (2017) 1140–1146, <https://doi.org/10.1016/j.electacta.2017.07.077>.
- [108] J. Huang, Y. Liang, H. Hu, S. Liu, Y. Cai, H. Dong, M. Zheng, Y. Xiao, Y. Liu, Ultrahigh-surface-area hierarchical porous carbon from chitosan: acetic acid mediated efficient synthesis and its application in superior supercapacitors, *J. Mater. Chem. A* 5 (47) (2017) 24775–24781, <https://doi.org/10.1039/c7ta08046h>.
- [109] X. Tong, Z. Chen, H. Zhuo, Y. Hu, S. Jing, J. Liu, L. Zhong, Tailoring the physicochemical properties of chitosan-derived N-doped carbon by controlling hydrothermal carbonization time for high-performance supercapacitor application, *Carbohydr. Polym.* 207 (August) (2019) 764–774, <https://doi.org/10.1016/j.carbpol.2018.12.048>.
- [110] J. Zhou, H. Wang, W. Yang, S. Wu, W. Han, Sustainable nitrogen-rich hierarchical porous carbon nest for supercapacitor application, *Carbohydr. Polym.* 198 (June) (2018) 364–374, <https://doi.org/10.1016/j.carbpol.2018.06.095>.
- [111] Q. Wu, M. Gao, S. Cao, J. Hu, L. Huang, S. Yu, A.J. Ragauskas, Chitosan-based layered carbon materials prepared via ionic-liquid-assisted hydrothermal carbonization and their performance study, *J. Taiwan Inst. Chem. Eng.* 101 (2019) 231–243, <https://doi.org/10.1016/j.jtice.2019.04.039>.
- [112] F.W. Scheller, R. Hintsche, D. Pfeiffer, F. Schubert, K. Riedel, R. Kindervater, Biosensors: fundamentals, applications and trends, *Sensors Actuators B Chem.* 4 (1) (1991) 197–206, [https://doi.org/10.1016/0925-4005\(91\)80198-S](https://doi.org/10.1016/0925-4005(91)80198-S).
- [113] Z. Gao, L. Wang, R. Su, R. Huang, W. Qi, Z. He, A carbon dot-based 'off-on' fluorescent probe for highly selective and sensitive detection of phytic acid, *Bioelectron.* 70 (Aug. 2015) 232–238, <https://doi.org/10.1016/j.bio.2015.03.043>.
- [114] S. Moradi, K. Sadrjavadi, N. Farhadian, L. Hosseinzadeh, M. Shahlaei, Easy synthesis, characterization and cell cytotoxicity of green nano carbon dots using hydrothermal carbonization of Gum Tragacanth and chitosan bio-polymers for bioimaging, *J. Mol. Liq.* 259 (2018) 284–290, <https://doi.org/10.1016/j.molliq.2018.03.054>.
- [115] L. Wang, B. Li, F. Xu, X. Shi, D. Feng, D. Wei, Y. Li, Y. Feng, Y. Wang, D. Jia, Y. Zhou, High-yield synthesis of strong photoluminescent N-doped carbon nanodots derived from hydrosoluble chitosan for mercury ion sensing via smartphone APP, *Biosens. Bioelectron.* 79 (2016) 1–8, <https://doi.org/10.1016/j.bios.2015.11.085>.
- [116] P.K. Gupta, N. Pachauri, Z.H. Khan, P.R. Solanki, One pot synthesized zirconia nanoparticles embedded in amino functionalized amorphous carbon for electrochemical immunosensor, *J. Electroanal. Chem.* 807 (September) (2017) 59–69, <https://doi.org/10.1016/j.jelechem.2017.11.018>.
- [117] B. Rezaei, N. Irannejad, A.A. Ensafi, M. Dinari, Application of modified carbon quantum dots/multiwall carbon nanotubes/pencil graphite electrode for electrochemical determination of dextromethorphan, *IEEE Sensors J.* 16 (8) (2016) 2219–2227, <https://doi.org/10.1109/JSEN.2016.2517005>.
- [118] I.-L. Lee, Y.-M. Sung, C.-H. Wu, S.-P. Wu, Colorimetric sensing of iodide based on triazole-acetamide functionalized gold nanoparticles, *Microchim. Acta* 181 (5) (2014) 573–579, <https://doi.org/10.1007/s00604-013-1150-0>.
- [119] N. Bhuvanesh, K. Velmurugan, S. Suresh, P. Prakash, N. John, S. Murugan, T. Daniel Thangadurai, R. Nandhakumar, Naphthalene based fluorescent chemosensor for Fe²⁺-ion detection in microbes and real water samples, *J. Lumin.* 188 (2017) 217–222, <https://doi.org/10.1016/j.jlumin.2017.04.026>.
- [120] L.S.Cui SL, P. Liu, X.H. Su, Surveys in Areas of high risk of iodine deficiency and iodine excess in China, 2012–2014: current status and examination of the relationship between urinary iodine concentration and goiter prevalence in children aged 8–10 years, *Biomed. Environ. Sci.* 30 (2) (2017) 88–96, <https://doi.org/10.3967/bes2017.012>.
- [121] G. Liu, B. Li, Y. Liu, Y. Feng, D. Jia, Y. Zhou, Rapid and high yield synthesis of carbon dots with chelating ability derived from acrylamide/chitosan for selective detection of ferrous ions, *Appl. Surf. Sci.* 487 (May) (2019) 1167–1175, <https://doi.org/10.1016/j.apsusc.2019.05.069>.
- [122] J. Song, L. Zhao, Y. Wang, Y. Xue, Y. Deng, X. Zhao, Q. Li, Carbon quantum dots prepared with chitosan for synthesis of CQDs/auNPs for iodine ions detection, *Nanomaterials* 8 (12) (2018) 1043, <https://doi.org/10.3390/NANO8121043>.
- [123] M. Friedman, Antibiotic-Resistant Bacteria: Prevalence in Food and Inactivation by Food-Compatible Compounds and Plant Extracts, *J. Agric. Food Chem.* 63 (15) (Apr. 2015) 3805–3822, <https://doi.org/10.1021/acs.jafc.5b00778>.
- [124] Y. Chen, C. Tan, H. Zhang, L. Wang, Two-dimensional graphene analogues for biomedical applications, *Chem. Soc. Rev.* 44 (9) (2015) 2681–2701, <https://doi.org/10.1039/C4CS00300D>.
- [125] H.-R. J., F.-G.W.Yao-Wen Jiang, Ge Gao, Xiaodong Zhang, Antimicrobial carbon nanospheres, *Nanoscale* 9 (41) (2017) 15786–15795, <https://doi.org/10.1039/x0xx000>.
- [126] I. Matos, M. Bernardo, I. Fonseca, Porous carbon: a versatile material for catalysis, *Catal. Today* 285 (2017) 194–203, <https://doi.org/10.1016/j.cattod.2017.01.039>.
- [127] M.J. Lázaro, S. Ascaso, S. Pérez-Rodríguez, J.C. Calderón, M.E. Gálvez, M. J. Nieto, R. Moliner, A. Boyano, D. Sebastián, C. Alegre, L. Calvillo, V. Celorrio, Carbon-based catalysts: synthesis and applications, *Comptes Rendus Chim.* 18 (11) (2015) 1229–1241, <https://doi.org/10.1016/j.crci.2015.06.006>.
- [128] D.S. Su, S. Perathoner, G. Centi, Nanocarbons for the development of advanced catalysts, *Chem. Rev.* 113 (8) (Aug. 2013) 5782–5816, <https://doi.org/10.1021/cr300367d>.
- [129] Y. Yu, O.Y. Gutiérrez, G.L. Haller, R. Colby, B. Kabius, J.A. Rob van Veen, A. Jentys, J.A. Lercher, Tailoring silica–alumina-supported Pt–Pd as poison-tolerant catalyst for aromatics hydrogenation, *J. Catal.* 304 (2013) 135–148, <https://doi.org/10.1016/j.jcat.2013.04.009>.
- [130] Y. Ji, Y. Jeon, C. Lee, D.-H. Park, Y.-G. Shul, Y.-I. Cho, Design of active Pt on TiO₂ based nanofibrous cathode for superior PEMFC performance and durability at high temperature, *Appl. Catal. B Environ.* 204 (2017) 421–429, <https://doi.org/10.1016/j.apcatb.2016.11.053>.
- [131] Y.L. Zhang, J.L. Li, L. Zhao, X.L. Sui, Q.Y. Zhou, X.F. Gong, J.J. Cai, J.Z. Li, D. M. Gu, Z.B. Wang, Nitrogen doped carbon coated Mo modified TiO₂ nanowires (NC@MTNWs-F) with functionalized interfacial as advanced PtRu catalyst support for methanol electrooxidation, *Electrochim. Acta* 331 (2020), 135410, <https://doi.org/10.1016/j.electacta.2019.135410>.
- [132] R. Liu, D. Wu, X. Feng, K. Müllen, Nitrogen-doped ordered mesoporous graphitic arrays with high electrocatalytic activity for oxygen reduction, *Angew. Chemie Int. Ed.* 49 (14) (Mar. 2010) 2565–2569, <https://doi.org/10.1002/anie.200907289>.
- [133] G.A. Ferrero, K. Preuss, A. Marinovic, A.B. Jorge, N. Mansor, D.J.L. Brett, A. B. Fuentes, M. Sevilla, M.-M. Titirici, Fe-N-doped carbon capsules with outstanding electrochemical performance and stability for the oxygen reduction reaction in both acid and alkaline conditions, *ACS Nano* 10 (6) (Jun. 2016) 5922–5932, <https://doi.org/10.1021/acsnano.6b01247>.
- [134] M. Qiao, S.S. Meysami, G.A. Ferrero, F. Xie, H. Meng, N. Grobert, M.M. Titirici, Low-cost chitosan-derived n-doped carbons boost electrocatalytic activity of multiwall carbon nanotubes, *Adv. Funct. Mater.* 28 (16) (2018) 1–7, <https://doi.org/10.1002/adfm.201707284>.
- [135] M. Pirsahab, S. Moradi, M. Shahlaei, N. Farhadian, Application of carbon dots as efficient catalyst for the green oxidation of phenol: kinetic study of the degradation and optimization using response surface methodology, *J. Hazard. Mater.* 353 (2010) (2018) 444–453, <https://doi.org/10.1016/j.jhazmat.2018.04.038>.
- [136] I.F. Nata, C. Irawan, P. Mardina, C.-K. Lee, Carbon-based strong solid acid for cornstarch hydrolysis, *J. Solid State Chem.* 230 (2015) 163–168, <https://doi.org/10.1016/j.jssc.2015.07.005>.
- [137] L. Qin, H. Mao, C. Lei, Q. Wang, Z. Gao, The SO₃H-functionalized carbonaceous@ montmorillonite efficient heterogeneous catalyst for synthesis of trimethylolpropane from long-chain fatty acid, *Microporous Mesoporous Mater.* 289 (1) (2019) 109623, <https://doi.org/10.1016/j.micromeso.2019.109623>.
- [138] X. Ge, M. Ge, X. Chen, C. Qian, X. Liu, S. Zhou, Facile synthesis of hydrochar supported copper nanocatalyst for Ullmann C[*s*bdn] coupling reaction in water, *Mol. Catal.* 484 (October 2019) (2019) 110726, <https://doi.org/10.1016/j.mcat.2019.110726>.